

Department of Biomedical Sciences

University of Veterinary Medicine Vienna

Institute of Medical Biochemistry (Head: Univ.-Prof. Dr.rer.nat. Florian Grebien)

**Toxicity of Cannabidiol on Brain Cancer Cells and Murine  
Mesencephalic Primary Cultures under Inhibition of Glycolysis**

**BACHELOR THESIS**

for obtaining the degree

**Bachelor of Science (BSc.)**

of the University of Veterinary Medicine Vienna

Submitted by

Sophie Svatunek

Vienna, June 2020

**Supervisor:** Dipl.-Biol. Dr.rer.nat Rudolf Moldzio

**Reviewer:** Ao.Univ.-Prof. Dr.med.vet. Alois Strasser

# Danksagung

Ich möchte mich ganz herzlich bei meinem Betreuer, Dipl.-Biol. Dr.rer.nat Rudolf Moldzio, für die Betreuung meiner Bachelorarbeit bedanken. Danke für deine Zeit, deine Bemühungen, deine Tipps & Ratschläge sowie deine herzliche & unkomplizierte Art. Danke, dass du mir immer geholfen hast, wenn ich Fragen hatte und mir stets zur Seite gestanden bist.

Ein großes Dankeschön gilt Ing. Barbara Kranner, Christopher Krewenka, BSc. & Marcus Schefzig, BSc. Danke für eure Geduld, eure Zeit, euer stets offenes Ohr, euren unermüdlichen Einsatz und euren wundervollen Teamgeist, den ihr täglich aufs Neue ins Labor mitgebracht habt. Ein besonders großes Dankeschön gilt Marcus, der vor allem zu Beginn großartige Arbeit geleistet hat, um mir mit großer Hilfsbereitschaft bei jeglicher experimenteller Laborarbeit beiseite zu stehen.

Bei allen Mitgliedern des Instituts für Medizinische Biochemie möchte ich mich für die schöne Zeit bedanken! Danke für die wohlthuende Arbeitsatmosphäre und die Offenheit, mit der ich bei euch willkommen geheißen wurde!

Ein großes Dankeschön geht an meine Familie. Mama, Papa, ich danke euch für eure Liebe & Unterstützung. Ohne eure wohlbehütete Kinderstube wäre ich heute niemals dort angekommen, wo ich bin. Oma, Opa, danke, dass ihr immer für mich da seid und ich immer zu euch kommen kann. Patrick, danke, dass du mir während des Studiums stets eine große mentale Stütze warst und dass ich immer auf dich zählen kann.

Ohne euer Zutun wäre diese Arbeit niemals zustande gekommen.

# Table of content

<b>1. Introduction</b>	<b>6</b>
<b>1.1. The endocannabinoid system</b>	<b>6</b>
1.1.1. The cannabinoid receptors	6
1.1.2. Endocannabinoids	7
1.1.3. Phytocannabinoids	8
<b>1.2. Cannabidiol</b>	<b>9</b>
1.2.1. Cannabidiol, the new panacea	10
1.2.2. Toxic properties of Cannabidiol against cancer cells	11
1.2.3. Effects of Cannabidiol in neural cells	14
1.2.4. Effects of Cannabidiol on mitochondria	15
<b>1.3. Energy metabolism</b>	<b>16</b>
1.3.1. General principles	16
1.3.2. Energy metabolism in cancer cells	18
1.3.3. Inhibition of glycolysis by 2-deoxy-D-glucose	19
<b>1.4. Cell culture</b>	<b>19</b>
1.4.1. Neural primary cells	20
1.4.2. Neural cell lines	20
<b>1.5. Aims of the study</b>	<b>21</b>
<b>2. Material and Methods</b>	<b>22</b>
<b>2.1. Material</b>	<b>22</b>
2.1.1. Animals	22
2.1.2. Chemicals	22
2.1.3. Equipment	23
<b>2.2. Methods</b>	<b>25</b>
2.2.1. Preparation of murine mesencephalic primary cells	25
2.2.2. Cultivation of murine mesencephalic primary cells	26
2.2.3. Anti-tyrosine-hydroxylase staining	28
2.2.4. Cultivation of murine and human cell lines	29
2.2.5. Preparation of murine and human cell lines	29
2.2.6. Lactate dehydrogenase activity determination	32
2.2.7. Resazurin reduction assay	33
2.2.8. BCA-Protein Assay	33
2.2.9. Statistics	34

<b>3. Results</b>	<b>35</b>
<b>3.1. 2-deoxy-D-glucose in glioma and neuroblastoma cells</b>	<b>35</b>
3.1.1. 2-deoxy-D-glucose in glioma	35
3.1.2. 2-deoxy-D-glucose in neuroblastoma	38
3.1.3. Comparison between metabolism of glioma and neuroblastoma upon treatment with 2-deoxy-D-glucose	41
<b>3.2. Cannabidiol in glioma and neuroblastoma cells</b>	<b>42</b>
3.2.1. Cannabidiol in glioma	42
3.2.2. Cannabidiol in neuroblastoma	45
3.2.3. Comparison between metabolism of glioma and neuroblastoma upon treatment with cannabidiol	48
<b>3.3. Cannabidiol and 2-deoxy-D-glucose in glioma and neuroblastoma cells</b>	<b>49</b>
3.3.1. Cannabidiol and 2-deoxy-D-glucose in glioma	49
3.3.2. Cannabidiol and 2-deoxy-D-glucose in neuroblastoma	52
3.3.3. Comparison between metabolism of glioma and neuroblastoma upon treatment with cannabidiol and 2-deoxy-D-glucose	55
<b>3.4. 2-deoxy-D-glucose in murine mesencephalic primary cells</b>	<b>56</b>
<b>4. Discussion</b>	<b>57</b>
<b>4.1. General remarks</b>	<b>57</b>
<b>4.2. 2-deoxy-D-glucose in glioma and neuroblastoma cells</b>	<b>57</b>
<b>4.3. Cannabidiol in glioma and neuroblastoma cells</b>	<b>59</b>
<b>4.4. Cannabidiol and 2-deoxy-D-glucose in glioma and neuroblastoma cells</b>	<b>60</b>
<b>4.5. 2-deoxy-D-glucose in murine mesencephalic primary cells</b>	<b>61</b>
<b>5. Conclusion</b>	<b>62</b>
<b>6. Summary</b>	<b>63</b>
6.1. English	63
6.2. German	64
<b>7. References</b>	<b>65</b>
<b>8. Appendix</b>	<b>74</b>
8.1. Figure Index	74
8.2. Table Index	77
8.3. Abbreviations	78

# 1. Introduction

## 1.1. The endocannabinoid system

The endocannabinoid system consists of two G-protein coupled receptors, which are called cannabinoid receptor type-1 (CB<sub>1</sub>) and cannabinoid receptor type-2 (CB<sub>2</sub>), their endogenous ligands and their enzymes which are responsible for the endocannabinoid metabolism (Di Marzo and Piscitelli 2015).

### 1.1.1. The cannabinoid receptors

The CB<sub>1</sub> receptor can be found abundantly in the central nervous system (CNS) and peripheral nervous system (PNS). Its density is especially high in the cerebellum, cortex, amygdala and basal ganglia. It is primarily expressed at the terminal ends of neurons, particularly glial cells and astrocytes, and initiates the inhibition of ongoing release of several inhibitory and excitatory neurotransmitters which are: acetylcholine, cholecystokinin, D-aspartate, dopamine, noradrenaline, glutamate, serotonin and  $\gamma$ -aminobutyric acid (GABA). Thus, appetite, cognition, emotion and locomotion are altered (Lambert 2009, 1–2; Pertwee 2008a; PubChem 21/05/2020; Williams and Kirkham 1999). It also promotes analgesia, decreases learning ability and is responsible for reward, which leads to the development of addictive behaviour for opiates (Brusberg et al. 2009; Howlett et al. 2002; Kauer and Malenka 2007).

The connection between the CB<sub>1</sub> receptor and the G<sub>i/o</sub>-protein subtype of G-proteins leads to an activation of K<sup>+</sup> channels and an inactivation of L-, N-, P- & Q-type voltage-gated Ca<sup>2+</sup> channels upon CB<sub>1</sub> receptor activation. Furthermore, this connection mediates tyrosine-phosphorylation of focal adhesion kinase, activation of mitogen-activated protein kinase (MAPK) and activation of phospholipase C $\beta$  which leads to a transient rise in intracellular Ca<sup>2+</sup> concentration. In addition, the activation of the CB<sub>1</sub> receptor stimulates the production of nitric oxide in different arterial and venous endothelial cells (Howlett et al. 2002).

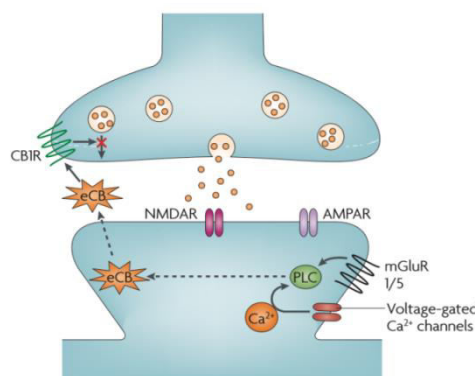


Figure 1. Activation of presynaptic CB<sub>1</sub> receptors leads to weakening of synaptic transmission (Kauer and Malenka 2007)

The CB<sub>2</sub> receptors can be divided into two isoforms: CB<sub>2A</sub> and CB<sub>2B</sub>. The CB<sub>2A</sub> receptor is expressed in the testis, muscles and the CNS, to be more precise in the cerebellum, cortex, amygdala, caudate, putamen and nucleus acumbens, and influences memory and learning. The CB<sub>2B</sub> isoform is predominantly expressed in the muscles, on immune cells and immune-related organs such as tonsil, spleen, thymus, lymph nodes and bone marrow, and influences inflammatory processes (Liu et al. 2009; Ratano et al. 2018).

Both, the CB<sub>1</sub> and CB<sub>2</sub> receptor, can alter the amount of intracellular cyclic adenosine monophosphate (cAMP) by inhibition or stimulation of the adenylyl cyclase (ADCY). This mechanism depends on the isoform of this enzyme. The ADCY isoforms 1, 3, 5, 6 & 8 get inhibited by the activation of CB<sub>1</sub> and CB<sub>2</sub> receptors, whereas the ADCY isoforms 2, 4 & 7 become stimulated by the activation of CB<sub>1</sub> and CB<sub>2</sub> receptors.

These two receptors share a sequence homology of 48 %. They also occur in several different species and reveal to have conserved domains. For example, the human and rodent CB<sub>1</sub> receptors share a high similarity of more than 97 % (Howlett et al. 2002).

### 1.1.2. Endocannabinoids

All molecules that are internally synthesized and can bind to the CB<sub>1</sub> and CB<sub>2</sub> receptors are referred to as endocannabinoids. Five different endocannabinoids are currently known: N-arachidonylethanolamine (anandamide), 2-arachidonoylglycerol (2-AG), noladin ether, virodhamine and N-arachidonoyl-dopamine.

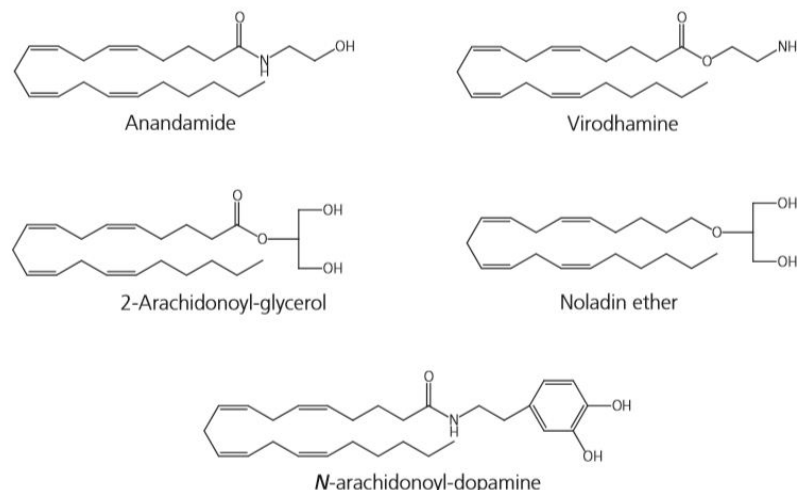


Figure 2. All 5 known endocannabinoids (Bisogno 2008)

The two most studied of these are anandamide and 2-AG which are both derivatives of arachidonic acid, a polyunsaturated, essential fatty acid with a 20-C backbone and 4 cis-double bonds, that is synthesized from dietary linoleic acid. These two endocannabinoids are

produced and released “on demand”, following an intracellular rise in  $\text{Ca}^{2+}$  concentration. (National Center for Biotechnology Information 19/03/2020; Bisogno 2008). Anandamide is described to be a partial agonist of both  $\text{CB}_1$  and  $\text{CB}_2$  receptors. Besides, it can also bind to other receptor types as for example the G-Protein coupled receptor 55 (GPR55), the transient receptor potential cation channel subfamily 5 member 1 (TRPV1) or the peroxisome proliferator-activated receptor  $\alpha$  and  $\gamma$  (PPAR $\alpha$  and PPAR $\gamma$ , respectively). The GPR55 is involved in pain and inflammation and promotes stem cell proliferation. PPAR $\alpha$  and PPAR $\gamma$  act as intracellular receptors for fatty acids and cholesterol-lowering drugs. The TRPV1 is also known as vanilloid receptor 1 or capsaicin receptor and mediates pain perception and long-term depression in the hippocampus and nucleus accumbens (Hill et al. 2018; Maccarrone et al. 2014; UniProt 22/03/2020, 22/03/2020, 22/03/2020, 22/03/2020). 2-AG exclusively acts on  $\text{CB}_1$  and  $\text{CB}_2$  receptors with a high efficacy and is therefore called a “real” endocannabinoid (Sugiura et al. 2006).

### 1.1.3. Phytocannabinoids

Cannabinoids are components of the plant *Cannabis sativa* which are analogues of terpenphenoles with a 21-C backbone. Their derivatives and transformation products are referred to as phytocannabinoids. More than 104 phytocannabinoids are currently known which can be clustered into eleven different types (Pertwee 2014, 3–4).

Chemical class	Number of compounds
(-)-delta-9-trans-tetrahydrocannabinol type	18
(-)-delta-8-trans-tetrahydrocannabinol type	2
cannabigerol type	17
cannabichromene type	8
cannabidiol type	8
cannabinodiol type	2
cannabielsoin type	5
cannabicyclol type	3
cannabinol type	10
cannabitriol type	9
miscellaneous-type cannabinoids	22
<b>Total cannabinoids</b>	<b>104</b>

Table 1. Constituents of *Cannabis sativa* by chemical class (adapted from Pertwee 2014)

The by far most popular phytocannabinoid of *Cannabis sativa* is certainly (-)-delta-9-trans-tetrahydrocannabinol ( $\Delta^9$ -THC) which has been discovered in the 1960s. Its synthetic analogue called nabilone (Cesamet, Valeant Pharmaceuticals, Aliso Viejo, CA, USA) is used for the therapy of vomiting and nausea caused by chemotherapy, for the induction of appetite in AIDS patients and for the relief of pain.  $\Delta^9$ -THC acts on both CB<sub>1</sub> and CB<sub>2</sub> receptors and is considered a partial agonist of these due to the fact that its synthetic analogues display a higher efficacy on them (Pertwee 2008b).

Phytocannabinoids are of great medical interest. They are considered potential therapeutics for Parkinson's Disease (PD), Alzheimer's Disease (AD), Amyotrophic Lateral Sclerosis, Autism Spectrum Disorders and Epilepsy. Due to its therapeutic properties, research has risen on one specific phytocannabinoid: Cannabidiol (Cifelli et al. 2020).

## 1.2. Cannabidiol

Cannabidiol (CBD) is a non-psychoactive constituent of *Cannabis* plants which can be found there abundantly. It produces a plethora of pharmacological effects that are of great therapeutical interest. It has got a very low affinity to both cannabinoid receptors, the CB<sub>1</sub> and CB<sub>2</sub> receptor, and moreover antagonises synthetic and natural cannabinoid receptor agonists like for example WIN55212 and CP55940. Besides, CBD has also been found to act as an inverse agonist of the CB<sub>2</sub> receptor. In addition, CBD acts as an agonist of the 5-hydroxytryptamine receptor 1A (5-HT<sub>1a</sub>), a type of serotonin receptor, which can be found in the CNS and PNS, and antagonises its agonist, serotonin, in a concentration-dependent matter. CBD also acts on the TRPV1, the transient receptor potential cation channel subfamily 5 member 2 (TRPV2) and on the transient receptor potential cation channel subfamily A member 1 (TRPA1) (Iannotti et al. 2014; Lambert 2009, 83–86). The TRPV2 belongs to the same protein-superfamily of the TRPV1, a target of the endocannabinoid anandamide, and is responsible for several mechanisms, for example pain perception, phagocytosis by microglia, insulin secretion and blood pressure control (Shibasaki 2016). The TRPA1 is likewise a member of the same protein-superfamily of the TRPV1 and TRPV2 and controls pain perception of endogenous inflammatory mediators such as the irritants of

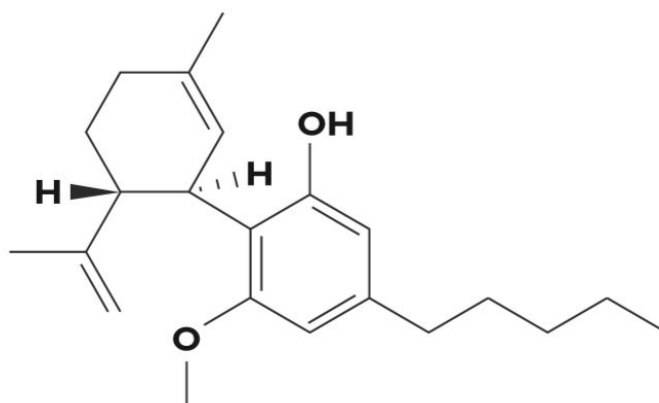


Figure 3. Structure of CBD (Massi et al. 2013)

garlic, wasabi and mustard, detects oxygen concentration and mediates cold perception (UniProt 13/04/2020). Furthermore, CBD acts as an antagonist of the GPR55 and an agonist of the PPAR $\gamma$  (Filippis et al. 2011; Ryberg et al. 2007).

CBD undergoes a first-pass effect in humans. Its metabolites are 7-hydroxy-CBD and CBD-7-oic acid, and they are eliminated via the urine. It displays a very low oral bioavailability of 6 – 31 %, a half-life period of 2 – 5 days when administered orally, a half-life period of 27 – 35 hours when inhaled and a half-life period of 18 – 33 hours when injected intravenously.

Several *in vitro* studies revealed that CBD is a potent inhibitor of plenty of cytochrome P450 enzymes (CYP), namely CYP1A2, CYP2B6, CYP2C9, CYP2D6 & CYP3A4. Thus, pharmacological interactions are highly probable (Zhornitsky and Potvin 2012).

### **1.2.1. Cannabidiol, the new panacea**

CBD influences several physiological processes, and thus is considered a potential therapeutic agent.

CBD has got an effect on cytokine production. When administered to lymph-node cells, CBD decreases the production of Interferon- $\gamma$ . Macrophages that received CBD decrease their Interleukin-10 production and increase their Interleukin-12 production. Synovial cells that were exposed to 5 mg CBD for 10 days decrease their production of tumor necrosis factor  $\alpha$  (TNF $\alpha$ ). Furthermore, intraperitoneal (i.p.) and subcutaneous (s.c.) injection of CBD at a concentration of 10 mg/kg blocked lipopolysaccharide-induced serum TNF $\alpha$  release.

CBD also maintains anti-oxidative properties. This feature may be relevant for the therapeutic treatment of neurodegenerative disorders like PD. The injection of the neurotoxic substance 6-hydroxydopamine (6-HD) into the medial forebrain *in vivo* leads to a significant reduction of dopamine and tyrosine-hydroxylase (TH) activity which can be considered a marker for dopaminergic neurons. The administration of CBD for 2 weeks after injection with 6-HD significantly reduces the number of damaged neurons by 6-HD. The immediate administration of CBD after 6-HD injection leads to a complete recovery of 6-HD-induced damage. In doing so, it upregulates the expression of Cu/Zn-superoxide dismutase which is a key enzyme in endogenous defense against oxidative stress.

Furthermore, the anti-oxidative properties of CBD seem to be likewise helpful for the treatment of AD. When CBD is administered to cultured rat pheocromocytoma PC12 cells prior to an exposure of  $\beta$ -amyloid peptide at a concentration of 1  $\mu$ g/ml, it significantly

reduces the production of reactive oxygen species (ROS), lipid peroxidation, caspase-3 levels, DNA-fragmentation and intracellular  $\text{Ca}^{2+}$  levels.

CBD has also been found helpful in cerebral ischemia. It decreased infarct volume after cerebral-artery occlusion. This effect can be inhibited by blocking the 5-HT<sub>1a</sub>.

CBD also maintains anxiolytic properties which could be shown in a placebo-controlled double-blind study (García-Arencibia et al. 2007; Lambert 2009, 85–96).

### 1.2.2. Toxic properties of Cannabidiol against cancer cells

Various reports of anticarcinogenic properties of CBD have been made.

CBD has shown the ability to reduce the metastatic spread and growth of breast carcinoma. Athymic mice and mice with a BalB/c background that received s.c. and i.p. injections of invasive human breast carcinoma cell lines show a less amount of lung metastasis and less tumour volume when receiving CBD for several days after the carcinoma-injection than those mice that did not receive anything after the carcinoma-injection (Ligresti et al. 2006). The mechanism behind the metastatic spread of breast carcinoma seems to involve the Id-1 gene. This gene encodes for a helix-loop-helix (HLH) protein which can form a heterodimer with the corresponding members of the HLH family of transcription factors and thus inhibits their transcription. Thereby, it regulates cell growth, senescence and cell differentiation and promotes metastasis of breast carcinoma cells. CBD has shown the ability to decrease the metastatic spread of human breast cell lines in a concentration-dependent manner by downregulation of the expression of the Id1 gene (McAllister et al. 2007; National Center for Biotechnology Information 02/04/2020).

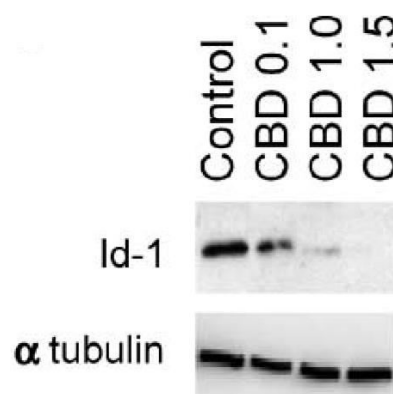


Figure 4. Western Blot Analysis of the expression of Id-1 with CBD at concentrations of 0.1, 1.0 & 1.5  $\mu\text{mol/l}$  (McAllister et al. 2007)

This downregulation is done by the upregulation of the active isoform of the extracellular signal-regulated kinase (ERK), a type of MAPK, than can lead to the inhibition of cell growth if its stimulus is long-lasting, and the production of ROS. Furthermore, CBD leads to the upregulation of the gene expression of the Id-2 gene. This gene is highly expressed in non-invasive breast carcinoma and is therefore considered a marker of good prognosis in breast cancer patients (McAllister et al. 2011). The cytotoxicity of CBD against breast cancer cells seems to be independent from the CB<sub>1</sub> and CB<sub>2</sub> receptor as well as the TRPV2. It rather induces autophagy as well as apoptosis via the intrinsic and the extrinsic pathway. Interestingly, the CBD-induced cell death can be reversed by using  $\alpha$ -tocopherol, a free radical scavenger, suggesting a pivotal role of ROS production in CBD-induced cytotoxicity against cancer cells. In addition, the AKT/mTor/4EBP1 pathway is a cell signaling pathway that is frequently dysregulated and overexpressed in many cancer types. It facilitates the expression of many proto-oncogenic proteins such as cyclin D1. CBD-treated cancer cells show a decreased PI3K/AKT/mTOR signaling and a less amount of cyclin D1 than untreated cancer cells (Shrivastava et al. 2011).

*In vivo* studies with athymic mice revealed that CBD also leads to a significant decrease in the metastatic spread of lung cancer cells in comparison with vehicle-treated mice. A decrease in cancer cell viability in a concentration-dependent matter can likewise be seen in cell culture when cells are incubated with CBD. This mechanism seems to be mediated by tissue inhibitors of matrix metalloproteinases-1 (TIMP1), which are normally responsible for the inhibition of matrix metalloproteinases. TIMP1 levels correlate inversely with the metastatic capacity of cancer cells and a high amount of TIMP1 can be found in CBD-treated cancer cells. Beyond that, the MAPK p38 and p42/44 have already been reviewed as upstream signaling molecules that lead to the induction of TIMP1. Indeed, the inhibition of p38 and p42/44 prior to CBD-treatment leads to a significant reduction of TIMP1 concentration and enhances the metastatic capacity *in vitro*. Next, inhibition of the CB<sub>1</sub>, CB<sub>2</sub> and TRPV1 receptors diminishes the CBD-mediated cytotoxic effects (Ramer et al. 2010a; Ramer et al. 2010b).

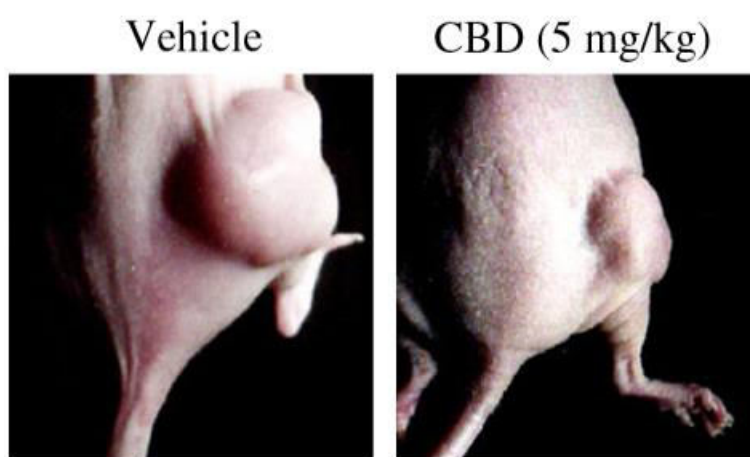


Figure 5. Tumour size of inoculated A549 lung cancer cells after treatment with CBD or a vehicle for up to 42 days (Ramer et al. 2010b)

The induction of apoptosis by CBD in tumours of the hematopoietic and lymphoid tissues of murine and human origin has also been reported both *in vivo* and *in vitro*. The CB<sub>2</sub> receptor seems to play a crucial role in the CBD-mediated cell death in this cancer, in marked contrast to several other cancer types, because selective CB<sub>2</sub> receptor-antagonists are able to reverse the cytotoxic effects of CBD (McKallip et al. 2006).

CBD also possesses antineoplastic properties against gliomas. Gliomas are tumours of glial origin and are frequently very invasive, proliferative and resistant to radio- & chemotherapy (Massi et al. 2013). To assess the anti-proliferative properties of CBD, athymic mice received s.c. injections of U87 glioma cell lines and were divided into 2 groups: Those that were treated with CBD peritumourally and those that were treated with a vehicle peritumourally. The CBD-treated mice showed a smaller tumour size on average after 12 to 23 days after treatment than those mice that did not receive anything after the tumour injection (Massi et al. 2004). CBD also reduced cell migration in the U87 human glioma cell line in a concentration-dependent manner. This effect could not be stopped by blocking the G<sub>i/o</sub>-protein subtype of G-proteins, suggesting no involvement of endocannabinoid receptors (Vaccani et al. 2005). Additionally, CBD seems to act specifically cytotoxic on brain tumours but at the same time does not harm the healthy neurons. The human glioma cell line U87 and primary glial cells have been tested on 10 and 25 µM of CBD. The experiment revealed that 25 µM CBD rises the intracellular levels of caspase-3, caspase-8 and caspase-9 and thus induces apoptotic cell death in U87 cells. Moreover, a significant depletion of glutathione and a time-dependent increase in ROS has been detected in this glioma cell line. In contrast, CBD did not harm the primary glial cells up to a concentration of 50 µM (Massi et al. 2006). Furthermore, a reduction of the activity of 5-lipoxygenase (5-LO) and an enhanced activity of fatty acid amide hydrolase (FAAH) has been detected in CBD-treated U87 cancer cells *in vivo*. 5-LO is an enzyme that is responsible for the production of leukotrienes and the regulation of cell growth and death in the CNS, whereas FAAH degrades anandamide (Massi et al. 2008). What's more, a decreased activity of the AKT protein of the PI3K/AKT/mTOR signaling pathway, a reduced amount of the active isoform of ERK and decreased levels of hypoxia-inducible factor-1 subunit α, a transcription factor which is responsible for angiogenesis, can be found in CBD-treated U87 cells (Solinas et al. 2013).

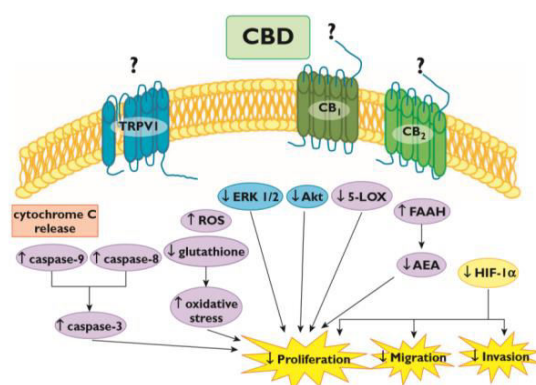


Figure 6. Effects of CBD on glioma cells (Massi et al. 2013)

### 1.2.3. Effects of Cannabidiol in neural cells

CBD also has an impact on neurotransmitter release in the CNS. It seems to alter the levels of the inhibitory GABA and the excitatory glutamate in the basal ganglia and the prefrontal cortex *in vivo*. A placebo-controlled, randomised, double-blind, repeated-measures, cross-over, case-control study revealed that CBD increases the concentration of GABA and glutamate in the basal ganglia and it increases the concentration of GABA in the prefrontal cortex, whereas it decreases the concentration of glutamate in the prefrontal cortex in healthy individuals (Pretzsch et al. 2019).

As mentioned previously, CBD acts as an agonist of the 5-HT<sub>1a</sub>. Thus, CBD mediates anxiolytic properties which could be proven *in vivo*. Male Wistar rats carried out a footshock chamber test. In this test the animals received an electrical shock when entering a dark chamber. Simultaneously, their freezing, rearing and crossing time as well as their heart rate were measured. The rats were divided into 2 groups: one group received CBD and the other group received a vehicle prior to the footshock test. The substances were injected directly into the bed nucleus of the stria terminalis via a stainless steel guide cannula. The experiment revealed that the CBD-treated rats show lesser freezing time, more crossings to the dark chamber, more rearing and a lower heart rate than those rats that received the vehicle. When the same experiment was conducted with a preliminary administration of a 5-HT<sub>1a</sub>-antagonist, WAY100635, to the CBD- or vehicle-treatment, the CBD-induced anxiolytic effects could be reversed (Gomes et al. 2012). The same results could be achieved in a restraint-experiment with male Wistar rats where CBD had been administered i.p. (Resstel et al. 2009).

It has also been reported that CBD acts on the mesolimbic system which is a neuronal system that is responsible for reward and drug abuse.

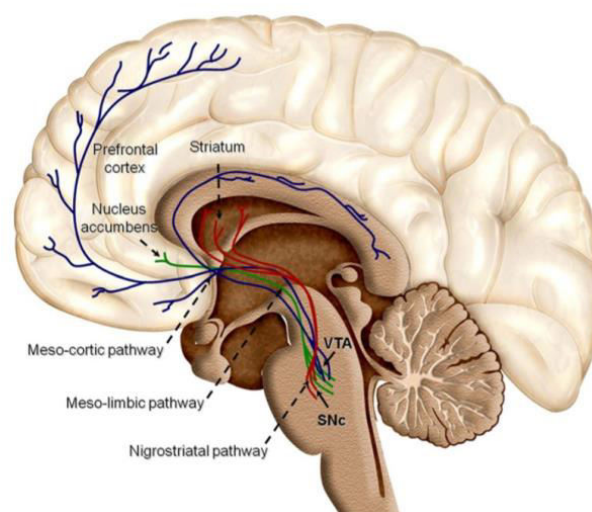


Figure 7. Anatomical structures of the mesolimbic system (Arias-Carrión et al. 2010)

Here, dopaminergic transmission is conducted. The dopaminergic neurons originate from the ventral tegmental area and the substantia nigra of the mesencephalon. Their axons project to the striatum and the prefrontal cortex. The dorsal part of the striatum consists of the caudate nucleus and the putamen, whereas the ventral part of the striatum is made up of the nucleus accumbens (Arias-Carrión et al. 2010).

The research on the effects of CBD on dopamine transmission has been contradictory. It could be demonstrated *in vivo* that CBD enhances the release of dopamine. Rats received CBD via microdialysis into the lateral hypothalamus. Thus, their dopamine levels in the nucleus accumbens increased for the following three hours after administration. Simultaneously, they showed enhanced wakefulness and a reduction in slow wave and rapid eye movement sleep (Murillo-Rodríguez et al. 2011). In contrast, CBD has also led to a reduced activity of dopaminergic neurons in the ventral tegmental area. When 100 ng CBD were infused into the ventral tegmental area of rats via a stainless steel guide cannula, a decrease in dopaminergic activity could be measured (Norris et al. 2016).

#### 1.2.4. Effects of Cannabidiol on mitochondria

The therapeutic properties of CBD seem to be at least partly conditioned by the alteration of mitochondrial activity. 16  $\mu$ M CBD is able to induce apoptosis via the release of cytochrome c and enhanced ROS production in isolated human monocytes in a concentration- and time-dependent matter.

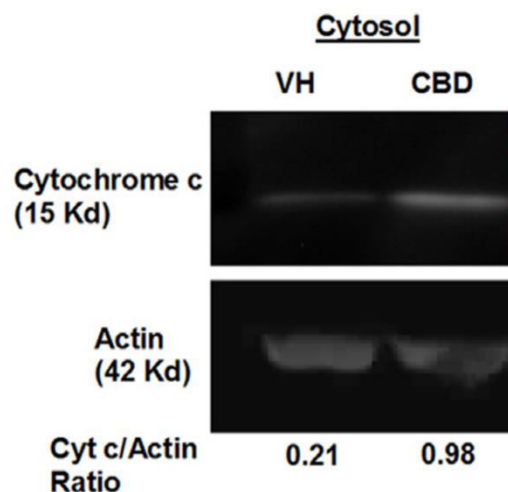


Figure 8. Western Blot Analysis of the amount of cytochrome c released into the cytosol of monocytes (Wu et al. 2018)

Moreover, it increases mitochondrial membrane potential and leads to a mitochondrial  $\text{Ca}^{2+}$  overload, following a rise in cytosolic  $\text{Ca}^{2+}$  and the oxidation of cardiolipin, a phospholipid that can be found abundantly in the inner mitochondrial membrane. Interestingly, the induction of apoptosis by CBD seems to be catalysed by the formation and opening of the mitochondrial permeability transition pore (MPTP) (Olivas-Aguirre et al. 2019; Wu et al. 2018). The MPTP is a protein located inside the mitochondria which is formed upon apoptotic or stressing stimuli. It is composed of a voltage-dependent anion channel (VDAC) of the outer mitochondrial membrane, an adenine nucleotide translocator of the inner mitochondrial membrane and cyclophilin D, a chaperone located in the mitochondrial matrix. These three proteins are normally disaggregated. But if an apoptotic or stressing stimulus is great enough, these proteins form a pore that is permeable for molecules up to a molecular weight of 1.5 kDa. The influx of such big molecules into the mitochondria leads to mitochondrial matrix swelling and cell death (Kalani et al. 2018). Indeed, it could be proven that the VDAC1, an isotype of the VDAC protein family, that is responsible for trans-membrane transport of adenosine triphosphate (ATP), is a direct target of CBD and is highly over-expressed in many human tumours (Rimmerman et al. 2013; Shoshan-Barmatz and Ben-Hail 2012; Shoshan-Barmatz et al. 2017).

### **1.3. Energy metabolism**

#### **1.3.1. General principles**

Energy metabolism in eukaryotes comprises the breakdown of nutrients such as fat, protein and saccharides as well as the production of energy carriers thereof and the production of biomolecules that are essential for various processes in living organisms such as nucleic acids and proteins. Due to the giant amount of chemical pathways that are involved in overall metabolism, the focus of this chapter is going to be the breakdown of saccharides and the subsequent generation of energy.

As saccharides are taken up by organisms, they are going to be broken up by enzymes inside the digestive system and will be absorbed into the cells. Glucose, a type of monosaccharide, will frequently undergo glycolysis which is a chemical pathway that leads to the generation of pyruvate and two molecules of ATP per molecule glucose. In general, pyruvate can be used in several chemical pathways. In the absence of sufficient oxygen levels, pyruvate will be reduced into lactate by the enzyme lactate dehydrogenase (LDH). Upon sufficient oxygen supply, pyruvate will become decarboxylated by the multi-unit enzyme pyruvate dehydrogenase (PDH) and the remaining molecule will be attached to coenzyme A which forms acetyl coenzyme A (acetyl-CoA).

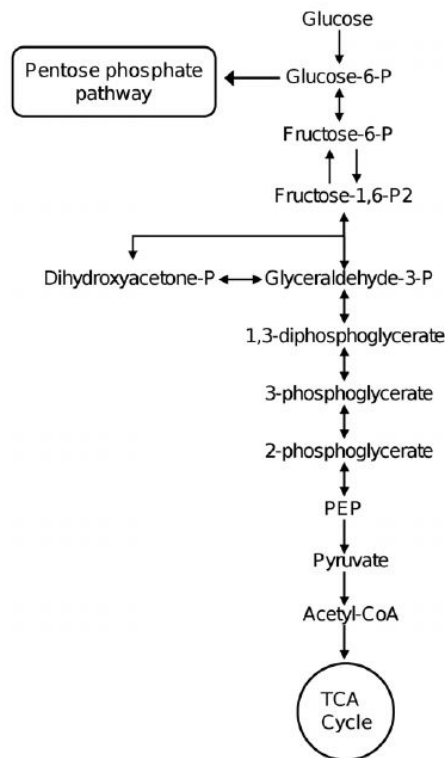


Figure 9. Overview of glycolysis (adapted from Phong et al. 2013)

Acetyl-CoA is involved in the initial step of the citric acid cycle (CAC). It will be imported into the mitochondrial matrix and consequently combines with oxaloacetate to form a citrate ion. Subsequently, this molecule will become decarboxylated and oxidized and forms  $\alpha$ -ketoglutarate. This process is referred to as “oxidative decarboxylation” and happens several times throughout the CAC, thereby producing nicotinamide adenine dinucleotide (NADH), flavin adenine dinucleotide ( $\text{FADH}_2$ ) and guanosine triphosphate (GTP). At the end of the CAC oxaloacetate is again produced and combines with another acetyl-CoA which in turn starts the cycle another time. The overall goal of the CAC is the generation of the electron carriers NADH,  $\text{FADH}_2$  and GTP.

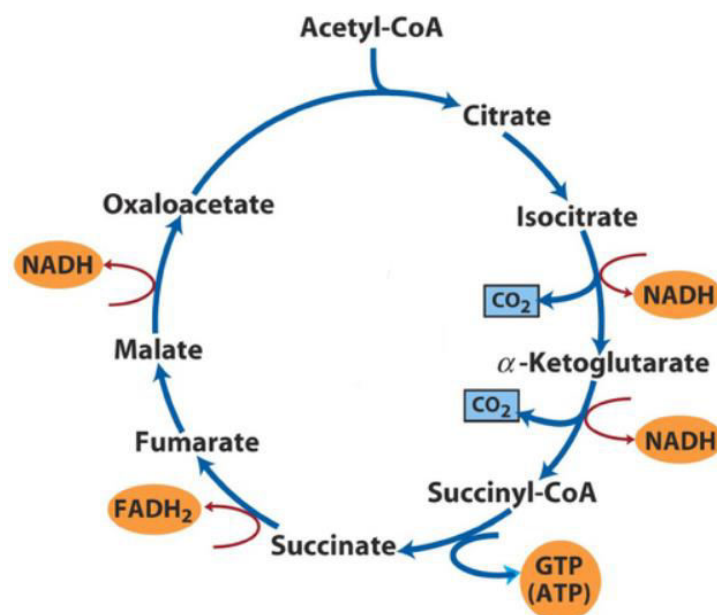


Figure 10. Overview of CAC (adapted from Salah Mohamed El Sayed et al. 2018)

Subsequently, NADH and FADH<sub>2</sub> will migrate to the four protein-complexes of the electron transport chain at the inner mitochondrial membrane in order to produce ATP and H<sub>2</sub>O as a by-product. They donate their electrons to the protein complexes I and II. These electrons will be transported across these four protein complexes and at the last complex, the electrons pair with O<sub>2</sub> to form H<sub>2</sub>O. The hereby generated energy drives H<sup>+</sup> ions into the intermembrane space. A surplus of H<sup>+</sup> ions within the intermembrane space is generated and this proton gradient drives the H<sup>+</sup> ions through an ATP-synthase within the inner mitochondrial membrane to the mitochondrial matrix. This shuttle of H<sup>+</sup> ions releases energy which is used for the production of ATP. This process of obtaining ATP by electron transport from NADH and FADH<sub>2</sub> to O<sub>2</sub> is called “oxidative phosphorylation” (Campbell and Farrel 2006; Voet et al. 1992).

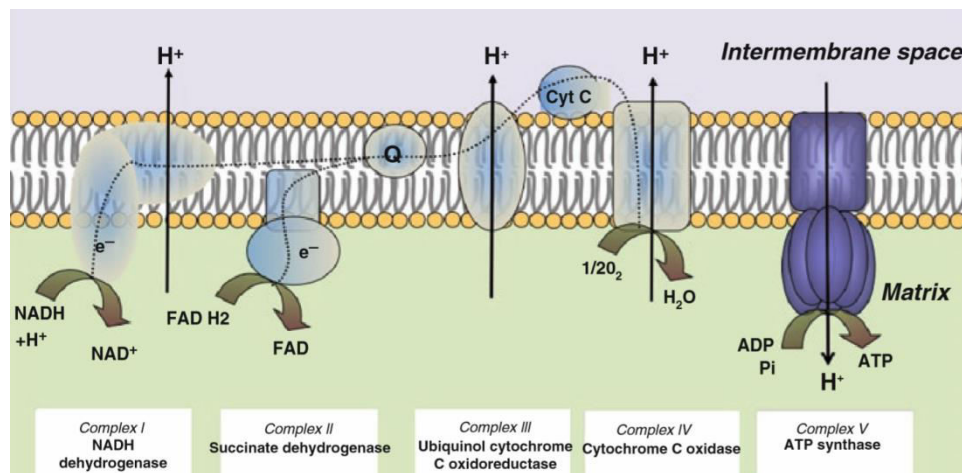


Figure 11. Overview of oxidative phosphorylation (adapted from Benard et al. 2011)

### 1.3.2. Energy metabolism in cancer cells

Cancer cells possess an altered energy metabolism. In the 1920s, the scientist Otto Warburg discovered that cancer cells had got an extensively high uptake of glucose in comparison to the surrounding tissue. Most of the glucose inside the cancer cells will not be used to produce energy via oxidative phosphorylation inside the mitochondria, but instead is used to produce a high amount of lactate. Even in the presence of sufficient oxygen supply, the majority of glucose will be converted into lactate. This phenomenon is called “Warburg effect” (Liberti and Locasale 2016). Clearly, the net gain of ATP of this pathway is lower than that of oxidative phosphorylation, but cancer cells avoid this drawback by enhancing the frequency of which glycolysis is conducted (Ganapathy-Kanniappan and Geschwind 2013). Indeed, inhibition of glycolysis has already proven to be a promising target for antineoplastic therapy (Korga et al. 2019; Le et al. 2010; Salah Mohamed El Sayed et al. 2018).

### 1.3.3. Inhibition of glycolysis by 2-deoxy-D-glucose

2-deoxy-D-glucose (2-DG) is a synthetic glucose analogue and acts as an effective and competitive inhibitor of glycolysis. In doing so, it enters the cell via glucose transporters and then competes for hexokinases. These enzymes are responsible for phosphorylation of hexoses and as a consequence thereof convert glucose to glucose-6-phosphate within the initial step of glycolysis. Thus, 2-DG becomes phosphorylated, cannot be metabolized any further and non-competitively blocks hexokinases. As a consequence, glucose cannot be metabolized any longer and glycolysis is stopped (Abdel-Wahab et al. 2019; Zhang et al. 2014).

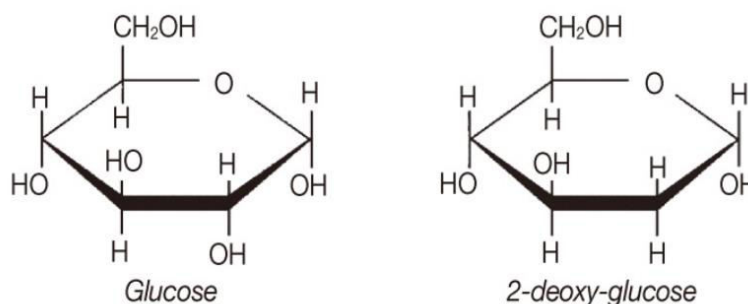


Figure 12. Comparison between glucose and 2-DG (adapted from Aghaee et al. 2012)

## 1.4. Cell culture

Cell culture is the process of growing cells under controlled conditions in a flask, petri dishes or culture plates. Thereby, proper gas supply, pH-value, temperature, osmotic pressure and nutrients must always be ensured. Additionally, antibiotics can be used in order to avoid contamination with bacteria.

Cell culture can be used by industry in order to produce commercially available biomolecules like e.g. hormones or blood coagulation factors and by research in order to investigate physiology and metabolism and to develop new pharmaceuticals like e.g. vaccines.

Cells that are obtained directly from a living organism and are sectioned into single cells before seeding are called "primary cell culture". Immortalised cells that can be grown in cell culture are named "cell lines". They are either obtained from a tumour or are synthetically immortalised by adding telomerase or oncogenes to the cells.

This technique is often referred to as growing cells "*in vitro*".

### 1.4.1. Neural primary cells

Neural primary cell culture is the cultivation of neural cells of living animals. This technique displays a great substitution to animal experiments and it allows us to study complex physiological processes in the nervous system that are simply inaccessible *in vivo*. The environment of the cells can easily be manipulated by adding substances to the culture medium or withdrawing substances from it. Thereby, the intrinsic cell response can readily be investigated. Despite of that, cell culture undergoes several limitations because sensory or cognitive response to specific stimuli cannot be addressed by this technique. Therefore, assessment of a whole animal is still required. Additionally, these cells have got a limited life time (Harry et al. 1998; Carter and Shieh 2015).

### 1.4.2. Neural cell lines

Cell lines provide several benefits such as they are cost effective, easy to handle, provide an unlimited supply of material and are compatible with our ethical concerns. They also provide a homologous population of cells and therefore consistent results can be achieved. Nevertheless, cell lines are genetically modified and thus, their metabolism and response to specific stimuli is probably not comparable to the real situation *in vivo*. Additionally, serial passage of the same cell line can lead to a genetic drift within the cells which consequently produces a more and more heterogeneous cell population (Kaur and Dufour 2012).

The cell lines I used in my thesis are the following: N18TG2 and U-87 MG.

The N18TG2 cells are a 6-thioguanine<sup>1</sup> resistant mutant of N18. This is a clonal cell line that is originally derived from a murine C13000 neuroblastoma<sup>2</sup> of an A/J strain male mouse (Cellosaurus 30/04/2020; Leibniz Institute DSMZ. German Collection of Microorganisms and Cell Cultures GmbH 30/04/2020; PubChem 30/04/2020; Tomolonis et al. 2018).

The U-87 MG cells are a human cell line which is originally derived from a glioma<sup>3</sup> of a female patient at the Uppsala University in Sweden in the 1960s. The original cell line became cross-contaminated with other cells of unknown origin and therefore the U-87 MG cell line only partly resembles the original donor (Allen et al. 2016; Cell Lines Service 01/05/2020).

---

<sup>1</sup> an analogue of guanine that is used for chemotherapy

<sup>2</sup> pediatric-onset cancer that originates from the sympathetic nervous tissue of the neural crest

<sup>3</sup> cancer of glial cells in the CNS

## 1.5. Aims of the study

The aim of this study was to investigate the effects of CBD on primary and cancer cells with a focus on the simultaneous inhibition of glycolysis since it has been reported to be a promising cancer therapy. Furthermore, the aim of this project was to elucidate, if the impact on primary and cancer cells differs from each other and if so, to which extent.

Taken together, following questions should be answered within this study:

- (1) Which concentration of 2-DG decreases overall cellular viability by 25 % in primary neural cells and cancer cells?
- (2) Which concentration of CBD acts cytotoxicly to primary neural cells and cancer cells?
- (3) Does the inhibition of glycolysis by 2-DG augment the toxic effect of CBD in primary neural cells and cancer cells?
- (4) Do the neuroblastoma and glioma cells react similarly to the treatment with 2-DG, CBD and CBD in combination with 2-DG?

Several different parameters were used in order to investigate the impact on our cells:

- ▶ Anti-TH-staining – Quantification of viable primary cells
- ▶ LDH activity determination – Quantification of dead cells
- ▶ Resazurin reduction assay – Measurement of overall cellular metabolism
- ▶ BCA-Protein assay – Quantification of living cells

## 2. Material and Methods

### 2.1. Material

#### 2.1.1. Animals

0F1/SPF mice, pregnant, Institute for Laboratory Zoology and Veterinary Genetics, Himberg, Austria

#### 2.1.2. Chemicals

2-deoxy-D-glucose (2-DG), Sigma-Aldrich, Germany

3,3'-diaminobenzidinetetrahydrochloride-hydrate (DAB) 97 %, Sigma-Aldrich, Germany

Absolute ethanol, Merck KGaA, Germany

Accustain, Sigma-Aldrich, Germany

Anti-TH mouse antibody, Szabo, Austria

B27 supplement minus AO 50x, Thermo Fisher Scientific, USA

Cannabidiol, THC Pharm, Germany

Colourless Dulbecco's modified eagle's medium (cDMEM) high glucose, Sigma-Aldrich, Germany

D-Glucose, Sigma-Aldrich, Germany

Dimethyl sulfoxide (DMSO), Merck KGaA, Germany

DNase 1 %, Sigma-Aldrich, Germany

Dulbecco's modified eagle's medium (DMEM) high glucose, Sigma-Aldrich, Germany

Dulbecco's modified phosphate buffered saline (DPBS) 1x, Thermo Fisher Scientific, USA

Foetal bovine serum, Sigma-Aldrich, Germany

Hank's balanced salt solution (HBSS) 1x, Thermo Fisher Scientific, USA

HEPES solution, Sigma-Aldrich, Germany

Horse serum, Sigma-Aldrich, Germany

Hydrogen peroxide (H<sub>2</sub>O<sub>2</sub>) 30 %, Merck KGaA, Germany

Kaiser's glycerol gelatine, Merck KGaA, Germany

L-Glutamine, Sigma-Aldrich, Germany

Nicotinamid adenine dinucleotide, Sigma-Aldrich, Germany

Peroxidase mouse IgG ABC-Kit, Vectastain, Vector Laboratories, USA

Pierce™ BCA Protein Assay Kit, Thermo Fisher Scientific, USA

Poly-D-lysine hydrobromide (PDL), Sigma-Aldrich, Germany

Resazurin sodium salt, Sigma-Aldrich, Germany

Ripa Lysis Buffer 10x, Merck KGaA, Germany

Sodium-pyruvate (Na-pyruvate), Sigma-Aldrich, Germany

Triton X, Roche Diagnostics, Germany

Trypan blue, Sigma-Aldrich, USA

Trypsin-EDTA 0.5 %, Thermo Fisher Scientific, USA

Tyrosin inhibitor soybean, Thermo Fisher Scientific, USA

### **2.1.3. Equipment**

48-well plates, Nunc, Denmark

96-well plates, Greiner bio-one, Germany

Cell culture flask 25 cm<sup>3</sup>, Greiner bio-one, Germany

Cell culture flask advanced 25 cm<sup>3</sup>, Greiner bio-one, Germany

Counting-chamber, Neubauer, Germany

Disposable syringe 5 ml, B. Braun, Germany

Easypet, Eppendorf, Germany

Examination gloves, Hartmann, Germany

Incubator, NAPCO Model 5410, Germany

Injection cannulas, B. Braun, Germany

Laminar Flow HERAsafe®, Kendro Laboratory Products, Germany

Microplate Reader Spark®, Tecan, Switzerland

Microscope, Nikon Diaphot 300, Japan

Multipette, Eppendorf, Germany

Multipurpose Container, Greiner bio-one, Germany

Petri dishes large, Nunc, Denmark

Petri dishes medium, Sterilin, UK

Petri dishes small, Nunc, Denmark

Pipette tips, Greiner bio-one, Germany

Reaction tubes, Greiner bio-one, Germany

Syringe filters, Whatman, UK

Vortex 1, IKA, Germany

Waterbath, GFL, Germany

## 2.2. Methods

### 2.2.1. Preparation of murine mesencephalic primary cells

A pregnant mouse was sacrificed on gestation day 14 in order to isolate neurons of the mesencephalon. Thus, one day before the preparation each well of two 48-well-plates was coated with 200  $\mu$ l of a PDL:DPBS-dilution (1:20). PDL is a synthetic chemical that serves as an adhesion molecule for the seeded cells because it reduces the surface tension inside each well. Additionally, the required instruments were autoclaved.

On the day of the preparation, the PDL:DPBS-dilution was removed, then each well was washed with 200  $\mu$ l of DPBS and finally 300  $\mu$ l DMEM were put into each well. Next, the required equipment and solutions were prepared as follows:

3 large petri dishes	10 ml DPBS (1x) / petri dish
4 medium petri dishes	4 ml DPBS (1x) / petri dish
1 small petri dish	1 drop of DPBS (1x)
Trypsin solution	1 ml Trypsin-EDTA (0.5 %) + 9 ml DPBS (1x)
Trypsin-inhibitor solution	1 mg Trypsin-inhibitor soybean + 4 ml DPBS (1x)
HBSS + DNase	2.5 ml HBSS (1x) + 50 $\mu$ l DNase (1 %)
Basic Medium (BM)	see page 27

Table 2. Overview of how the required equipment and solutions were prepared for the preparation of the pregnant mouse

Afterwards, the solutions were put into the incubator. All petri dishes, except for one large, and the sterile instruments were put into the laminar flow.

Then, the mouse was anaesthetised with CO<sub>2</sub> and sacrificed by cervical dislocation. Subsequently, the abdomen was rinsed with ethanol (70 %) and opened. The uterus was earned with a scissors and transferred to a large petri dish. The petri dish was covered and brought into the laminar flow. Thus, all further steps were conducted under sterile conditions. Then, the embryos were extricated from the uterus and their placenta and were put into the second large petri dish. There, the extraembryonic membranes were removed. Next, the embryos were transferred into a medium petri dish and were cut in half. The upper halves were put into the second medium petri dish. The skulls were opened with a scissors and a

small forceps before the brains were removed and brought into the third medium petri dish. Then, the prosencephala and myelencephala were removed and the mesencephala were put into the fourth medium petri dish. The meninges were removed and the mesencephala were transferred into the small petri dish.

Next, the mesencephala were cut several times with a scissors. Subsequently, 1 ml trypsin solution was added to the petri dish and this mix was put into a multipurpose container. Then, 1 ml trypsin solution and 2 ml HBSS + DNase were added to the multipurpose container and subsequently, it was put into the waterbath where it remained for 7 minutes at 36°C.

Afterwards, the multipurpose container was put into the laminar flow. 2 ml trypsin-inhibitor solution were added. Next, it was centrifuged at 100 g for 4 minutes.

3 ml BM and 50 µl DNase were added to the multipurpose container. Next, trituration was conducted with fire polished pasteur pipettes and then the mixture remained standing for 10 minutes. In the meantime, 6 ml BM were put into a culture medium flask which then was incubated at 37°C and 5 % CO<sub>2</sub>. Then, 3 ml of the supernatant of the multipurpose container were put into the flask and it was brought into the incubator. 3 ml BM and 50 µl DNase were again added to the multipurpose container, the solution became trituated with fire polished pasteur pipettes, it remained standing for 10 minutes and another 3 ml of the supernatant were added to the multipurpose container. These steps were repeated for another time which yields in a total of 3 triturations and a sum of 15 ml inside the flask (6 ml BM + 3 ml supernatant + 3 ml supernatant + 3ml supernatant = 15 ml).

The cells inside the flask were counted with trypan blue and a counting chamber. Subsequently, they became diluted with BM to a final concentration of 750 000 cells/ml.

The DMEM of the 48-well plates was discarded and 340 µl of cell suspension were added to each well. Finally, the plates were put into the incubator.

### **2.2.2. Cultivation of murine mesencephalic primary cells**

The primary mesencephalic cells were cultivated for a total of 15 days. On day 12, the experiment was conducted, and on day 14 and 15, the staining was performed. The cells were incubated at 37°C and 5 % CO<sub>2</sub> until day 13.

The used mediums for the cultivation of the primary mesencephalic cells were prepared as follows:

BM	N4
50 ml DMEM	50 ml cDMEM
500 µl HEPES solution (1 M)	500 µl HEPES solution (1 M)
370 µl glucose solution (20 %)	370 µl glucose solution (20 %)
1 ml L-glutamine (200 mM)	1 ml L-glutamine (200 mM)
5 ml foetal bovine serum	1 ml B27 supplement (50x)

Table 3. Composition of BM and N4

On the day of the preparation, 340 µl of cell suspension were added to each well. From now on, 300 µl of medium were changed on the required days. On day 5, BM and N4 were 1:2 mixed in a flask before they were used for cultivation.

Day	Schedule
0	harvest
1	change of BM
3	change of BM
5	switch of BM to BM/N4
6	change of N4
8	change of N4
10	switch of N4
12	experiment
14	Anti-TH staining, part 1
15	Anti-TH staining, part 2

Table 4. Overview of how mesencephalic primary cells were cultivated for 15 days

### 2.2.3. Anti-tyrosine-hydroxylase staining

On day 14 and 15, the mesencephalic primary cells were stained for the detection of dopaminergic neurons. Therefore, the anti-TH antibody staining was used with diaminobenzidine development. This staining leads to a brown dye of dopaminergic neurons. These neurons contain the enzyme TH which catalyses the conversion of the amino acid L-tyrosine into levodopa which is the precursor of the neurotransmitter dopamine.

On day 14, the N4 medium was discarded and 0.2 ml Accustain were added to each well with a multipette for cell fixation. After 15 minutes, the Accustain was replaced with 0.2 ml Triton X solution (0.4 %, mixed with DPBS) per well for 30 minutes to perforate the cell membrane. Next, each well was washed with 0.2 ml DPBS for 3 times, in which the DPBS remained inside each well for 2 minutes. The DPBS was finally discarded and 0.2 ml horse serum (1:50 dilution, mixed with DPBS) were added to each well and remained for 1.5 hours. The anti-TH mouse antibody was 1:1000 diluted with horse serum mixture. Finally, the horse serum was discarded and 0.2 ml anti-TH mouse antibody horse serum mixture was added to each well. Finally, the plates were put into the refrigerator at 4°C and remained over night.

On day 15, the supernatant of each well was discarded and they were washed with 0.2 ml DPBS for 3 times, in which the DPBS remained inside each well for 2 minutes. The DPBS was finally discarded and 0.2 ml biotinylated horse anti-mouse IgG (1:400 dilution, mixed with DPBS) was added to each well where it remained for 1.5 hours. Subsequently, a solution of avidin and biotin were prepared. 1 drop of each were initially mixed. Then 5 ml of DPBS were added. This mixture was shaken and remained like this for at least 30 minutes. After the 1.5 hours passed, the supernatant of each well was discarded. The wells were washed with 0.2 ml DPBS for 3 times, in which the DPBS remained inside each well for 5 minutes. Then, 0.2 ml avidin-biotin-solution was added to each well and remained for 1.5 hours. Subsequently, wells were washed with 0.2 ml DPBS for 3 times, in which the DPBS remained inside each well for 5 minutes. In the meantime, the DAB-solution was prepared. First, 20 µl H<sub>2</sub>O<sub>2</sub> and 500 µl DPBS were mixed. Second, 10 mg DAB, 10 ml DPBS and 100 µl of the previously prepared solution were mixed and shaken. 0.2 ml of this solution was added to each well after the washing step. After 5 – 10 minutes the supernatant of each well was discarded. The wells were washed with 0.2 ml DPBS for 3 times, in which the DPBS remained inside each well for 2 minutes. Finally, the cells were coated with Kaiser's glycerol gelatine which had been heated inside the waterbath at 50°C for at least 10 minutes.

The dopaminergic neurons then appeared brown under the microscope. The number of dopaminergic neurons was then determined through counting them at 100x magnification of Nikon Diaphot 300 microscope.

#### 2.2.4. Cultivation of murine and human cell lines

The N18TG2 and U-87 MG were permanently incubated at 37°C and 5 % CO<sub>2</sub> in cell culture flasks. The cells were split on Monday, Wednesday and Friday with maintaining-medium (MM). The N18TG2 were split 1:10, whereas the U-87 MG were split 1:5 – 1:3.

On Tuesday, cells were prepared for experiments. Therefore, the MM was discarded and the cells were harvested with treatment-medium (TM).

MM	TM
44 ml DMEM	48 ml cDMEM
5 ml foetal bovine serum	1 ml B27 supplement (50x)
1 ml Na-pyruvate (100 mM)	1 ml Na-pyruvate (100 mM)
1 ml L-glutamine (200 mM)	1 ml L-glutamine (200 mM)

Table 5. Composition of MM and TM

#### 2.2.5. Preparation of murine and human cell lines

200 µl of a PDL:DPBS-dilution (1:20) were put in each well of the 48-well-plate 24 hours before cells were going to be seeded into the plate. The plate was put into the incubator at 37°C and 5 % CO<sub>2</sub> and remained over night.

On the day of the experiment, the PDL:DPBS-dilution was discarded. The wells were washed with 200 µl DPBS and subsequently, 200 µl cDMEM were added to each well. The plate was put into the incubator until cells were going to be seeded into the wells. Then, the cDMEM was discarded and cell suspension was added to each well.

First, the determination of the toxicity of 2-DG was desired. Therefore, the plates were prepared and the cells were harvested as previously described and put onto plates as follows:

<b>N18TG2</b>	<b>U-87 MG</b>
96-well-plate	48-well-plate
400 000 cells/ml	300 000 cells/ml
75 $\mu$ l per well	150 $\mu$ l per well

Table 6. Overview of how cells were seeded for the determination of the toxicity of 2-DG

The appropriate dilutions of 2-DG were prepared as follows. The 50mM-dilution was filtered sterilely before the subsequent dilutions were made.

<b>doubled concentration</b>	<b>concentration inside each well</b>	<b>2-DG</b>	<b>TM</b>
50 mM	25 mM	41.04 mg	5000 $\mu$ l
30 mM	15 mM	900 $\mu$ l [50 mM]	600 $\mu$ l
20 mM	10 mM	1100 $\mu$ l [50 mM]	1650 $\mu$ l
10 mM	5 mM	1125 $\mu$ l [20 mM]	1125 $\mu$ l
5 mM	2.5 mM	750 $\mu$ l [10 mM]	750 $\mu$ l
0 mM	0 mM	-	1500 $\mu$ l

Table 7. The tested dilutions of 2-DG

Then, 75  $\mu$ l and 150  $\mu$ l of the appropriate 2-DG-dilution were added to each well of the 96-well-plate and 48-well-plate, respectively. The cells were measured after 24 and 48 hours. The LDH activity determination, the resazurin reduction assay and the BCA-Protein Assay were used in order to determine the cell viability.

Second, the effect of CBD alone and under inhibition of glycolysis by 2-DG was tested. Therefore, the plates were prepared and the cells were harvested as previously described and put onto plates as follows:

<b>N18TG2</b>	<b>U-87 MG</b>
96-well-plate	48-well-plate
100 000 cells/ml	75 000 cells/ml
150 $\mu$ l per well	300 $\mu$ l per well

Table 8. Overview of how cells were seeded for the CBD-experiment

The cells were incubated for 24 hours at 37°C and 5 % CO<sub>2</sub>. On the next day, the appropriate dilutions for CBD and 2-DG were prepared. A 25 mM stock of CBD in DMSO was kept at -20°C. Thus, a control medium (CM) was prepared as follows in order to keep the concentration of DMSO inside every well constant: 12  $\mu$ l DMSO were diluted in 2988  $\mu$ l TM. 2400  $\mu$ l of this dilution was mixed with another 9600  $\mu$ l TM.

<b>doubled concentration</b>	<b>concentration inside each well</b>	<b>CBD</b>	<b>CM</b>
20 $\mu$ M	10 $\mu$ M	see below	see below
2 $\mu$ M	1 $\mu$ M	170 $\mu$ l [20]	1530 $\mu$ l
0.2 $\mu$ M	0.1 $\mu$ M	170 $\mu$ l [2]	1530 $\mu$ l
0.02 $\mu$ M	0.01 $\mu$ M	150 $\mu$ l [0.2]	1350 $\mu$ l
0 $\mu$ M	0 $\mu$ M	-	3000 $\mu$ l

Table 9. The tested dilutions of CBD

The 20  $\mu$ M CBD-dilution was prepared as follows: 8  $\mu$ l of frozen CBD were diluted in 1992  $\mu$ l TM. 480  $\mu$ l of this dilution was mixed with another 1920  $\mu$ l TM.

The appropriate 2-DG dilution was prepared as follows:

doubled concentration	concentration inside each well	2-DG	TM
20 mM	10 mM	32.832 mg	10 000 $\mu$ l

Table 10. The appropriate 2-DG dilution for the CBD-experiment

The supernatant of each well was discarded. First, 75  $\mu$ l and 150  $\mu$ l of the appropriate CBD-dilution were added to each well of the 96-well-plate and 48-well-plate, respectively. Second, 75  $\mu$ l and 150  $\mu$ l of the appropriate 2-DG-dilution or TM were added to each well of the 96-well-plate and 48-well-plate, respectively. The cells were measured after 24 and 48 hours. The LDH activity determination, the resazurin reduction assay and the BCA-Protein Assay were used in order to determine the cell viability.

### 2.2.6. Lactate dehydrogenase activity determination

LDH is an enzyme that can reduce pyruvate into lactate by oxidation of NADH upon insufficient oxygen supply within glycolysis. When cells are damaged and undergo apoptosis or necrosis, LDH is released into the surrounding fluid. The release of LDH into the fluid can be measured through the consumption of NADH which is directly proportional to the number of lysed cells.

The measurement was performed after 24 and 48 hours of incubation of the tested substances. NADH and Na-pyruvate were diluted in LDH-buffer as follows:

LDH-buffer	LDH-buffer for experiment
100 ml DPBS (1x) + 2 ml HEPES solution (1 M)	15 ml LDH-buffer + 1.92 mg NADH + 1.023 mg Na-pyruvate

Table 11. Overview of how chemicals were prepared for the determination of LDH activity

50  $\mu$ l of cell suspension were put into a new 96-well plate. 85  $\mu$ l of LDH-buffer for experiment were put onto the 50  $\mu$ l of cell suspension. Subsequently, the cell suspension was measured at 334 nm, which is the absorption maximum of NADH, in Microplate Reader after 30, 60 and 90 seconds.

### 2.2.7. Resazurin reduction assay

In order to determine the cell viability, the resazurin reduction assay was used. Resazurin is a non-toxic, non-fluorescent, blue substance that is cell permeable. Once taken up by cells, resazurin will be reduced to the fluorescent and pink resorufin by NADH within viable mitochondria. The conversion of resazurin into resorufin can be seen by colour change and measured spectrophotometrically at their absorption maximum at 600 nm and 570 nm, respectively. Therefore, the amount of resorufin is a reliable indicator of cellular overall metabolism.

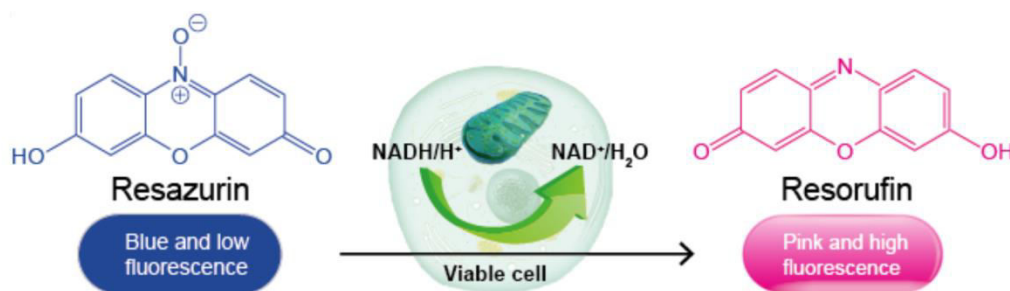


Figure 13. Reduction of resazurin into resorufin by viable cells (Creative Bioarray 22/04/2020)

The measurement was performed after 24 and 48 hours of incubation of the tested substances. First, 50  $\mu$ l of cell suspension were put into a new plate for the LDH activity determination. Second, 20  $\mu$ l and 50  $\mu$ l resazurin solution (500  $\mu$ M, mixed DPBS) were added to each well of the 96-well-plate and 48-well-plate, respectively. Cells were measured after 0, 1, 2 and 3 hours after addition of resazurin solution. Throughout this process, cells were incubated at 37°C and 5 % CO<sub>2</sub>.

### 2.2.8. BCA-Protein Assay

The amount of protein inside a well informs us about the amount of living cells inside it. Thus, the BCA-Protein Assay was used. It consists of the following two consecutive reactions: First, copper-(II)-ions react with at least two peptide bonds to form a chelate in an alkaline solution. Thereby, the copper-(II)-ion becomes reduced to a copper-(I)-ion. Second, two molecules of bicinchoninic acid (BCA) react with the previously formed copper-(I)-ion, which together appear as an intense-violet colour and have got an absorbance maximum at 562 nm.

The measurement was performed after 24 and 48 hours of incubation of the tested substances. The supernatant of each well was discarded. Subsequently, a 1:10-dilution of Ripa Lysis Buffer:distillated water was prepared and 200  $\mu$ l of this dilution was added to each well. Then, the cells were lysed for 15 minutes. Working reagent (WR) and the standard probes of bovine serum albumin (BSA) were prepared as follows:

<b>WR</b>
15 ml Reagent A + 0.3 ml Reagent B

Table 12. Composition of WR for BCA-Protein Assay

stock solution: 2000 µg/ml BSA		
	BSA	DPBS (1x)
<b>500 µg/ml</b>	50 µl [stock]	150 µl
<b>125 µg/ml</b>	50 µl [500]	150 µl
<b>50 µg/ml</b>	100 µl [125]	150 µl
<b>25 µg/ml</b>	100 µl [50]	100 µl
<b>0 µg/ml</b>	-	100 µl

Table 13. Composition of standard probes for BCA-Protein Assay

25 µl of each specimen and each standard probe were put into a new 96-well-plate. 200 µl WR were added to each well. The plate was put onto a plate shaker for 30 seconds and afterwards, it was incubated at 37°C and 5 % CO<sub>2</sub> for 30 minutes. Finally, the measurement was performed at 562 nm, the absorption maximum of the BCA/copper-complex.

### 2.2.9. Statistics

Data were obtained from at least 4 independent experiments, in which each condition was carried out as triplicate. Data are expressed as means ± standard deviation (SD). Statistical analysis was conducted with non-parametrical Kruskal-Wallis (H)-test followed by Chi<sup>2</sup>-test. For comparison of differences between the control group vs. the group that was treated with 2-DG alone, the non-parametric rank-sum test, Mann-Whitney-U-test, was used. P < 0.05 was considered as statistically significant and is displayed as (\*, #).

## 3. Results

### 3.1. 2-deoxy-D-glucose in glioma and neuroblastoma cells

#### 3.1.1. 2-deoxy-D-glucose in glioma

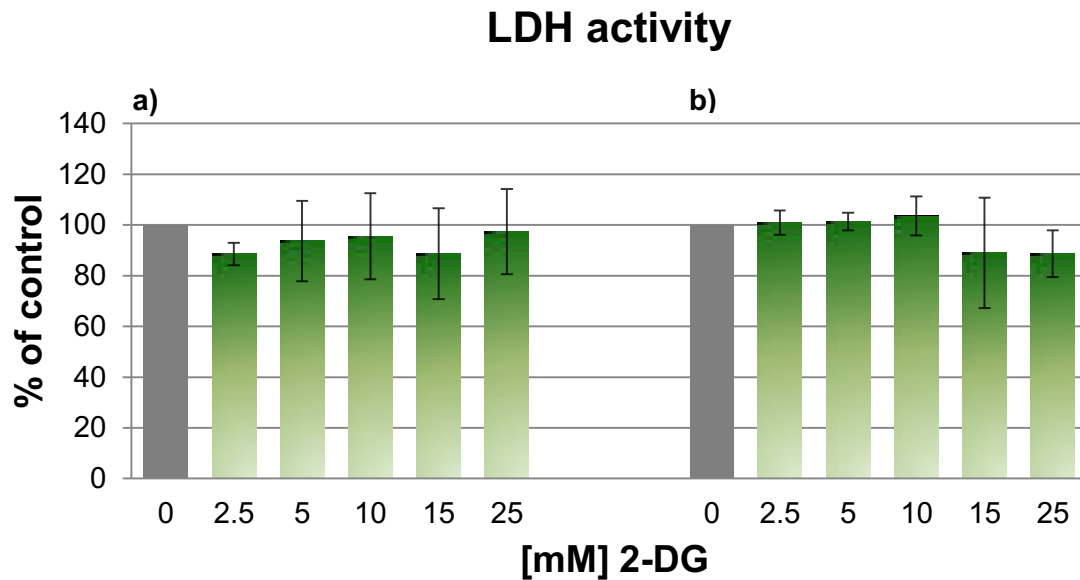


**Figure 14. LDH activity in U-87 MG glioma after exposure to 2-DG for (a) 24 hours and (b) 48 hours.** Data are expressed as means  $\pm$  SD of 4 independent experiments. Statistical evaluation does not reveal any significant changes.

No change in LDH activity of glioma cells occurred within the whole treatment with 2-DG. A slight decrease, by 10 %, can be seen at 15 mM and 25 mM 2-DG after 48 hours.

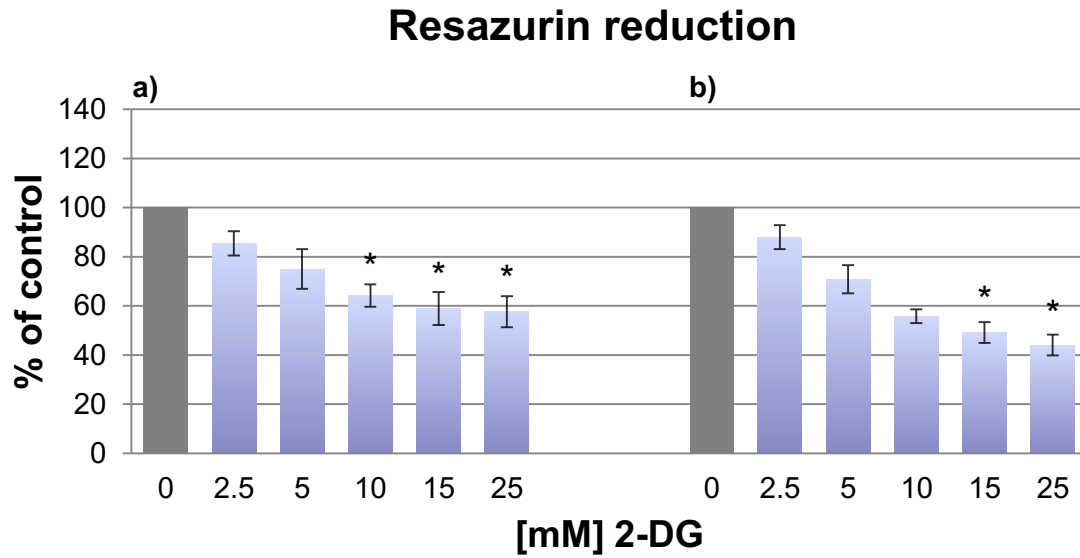


**Figure 15. Resazurin reduction in U-87 MG glioma after exposure to 2-DG for (a) 24 hours and (b) 48 hours.** Data are expressed as means  $\pm$  SD of 4 independent experiments.  $P < 0.05$  (\*) determined with Kruskal-Wallis (H)-test followed by Chi<sup>2</sup>-test.

A continuous decrease in resazurin reduction of glioma cells was observed after 24 and 48 hours. Although significant, the diminishment is greater after 48 hours than after 24 hours, whereat 15 mM and 25 mM display the highest diminishment to 49 % and 44 %, respectively.

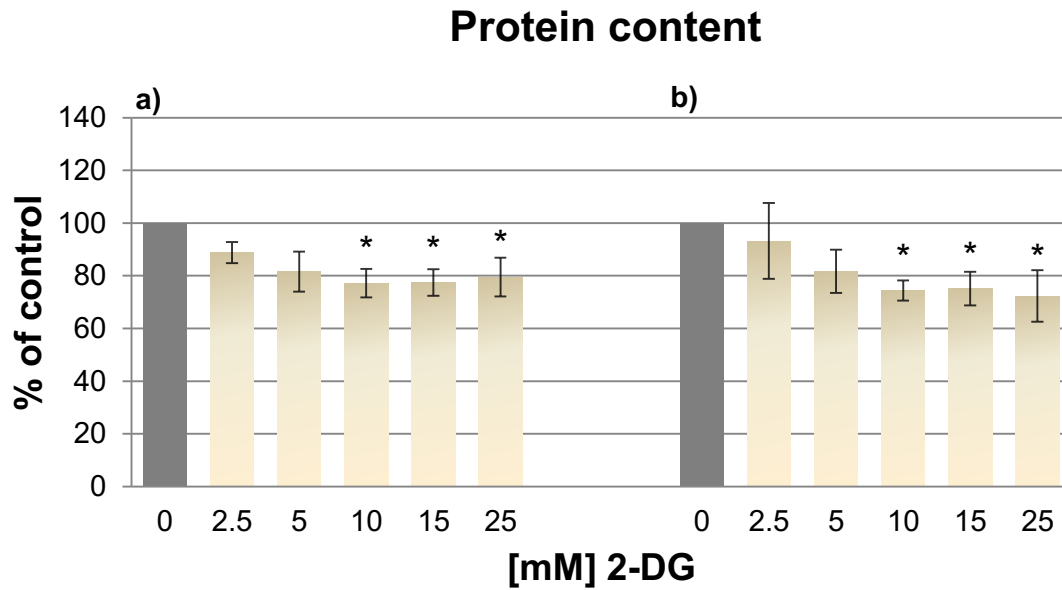


**Figure 16. Protein content in U-87 MG glioma after exposure to 2-DG for (a) 24 hours and (b) 48 hours.** Data are expressed as means  $\pm$  SD of 4 independent experiments.  $P < 0.05$  (\*) determined with Kruskal-Wallis (H)-test followed by Chi<sup>2</sup>-test.

A significant decrease in protein content of glioma cells was revealed for 10 – 25 mM after 24 and 48 hours. Interestingly, from 10 mM onwards, no real change in protein content can be detected.

### 3.1.2. 2-deoxy-D-glucose in neuroblastoma

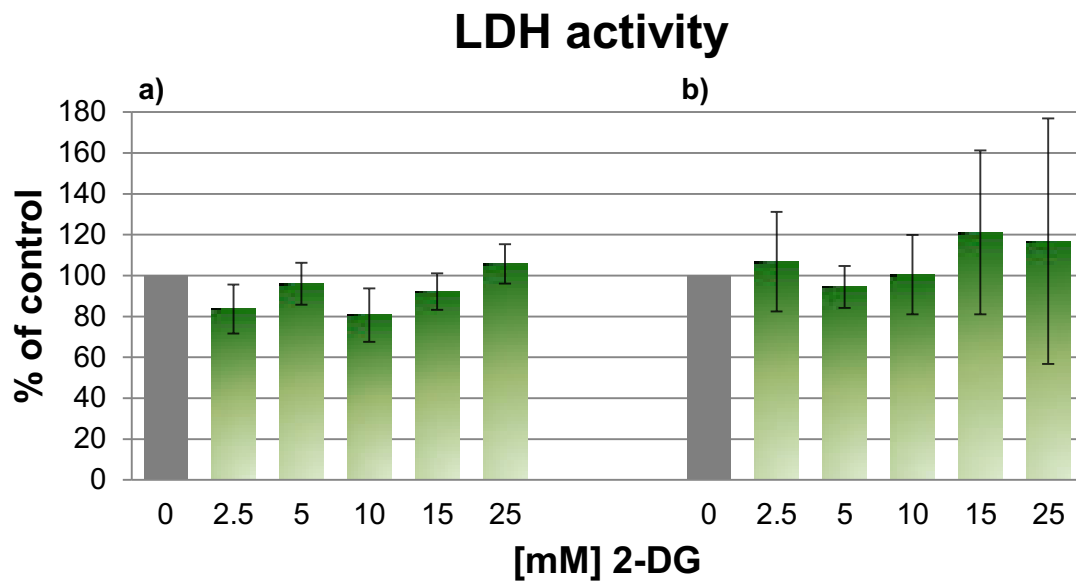


**Figure 17. LDH activity in N18TG2 neuroblastoma after exposure to 2-DG for (a) 24 hours and (b) 48 hours.** Data are expressed as means  $\pm$  SD of 4 independent experiments. Statistical evaluation does not reveal any significant changes.

LDH activity in neuroblastoma cells is unchanged in all conditions, but display a high variation with a maximum SD of 60 % at 25 mM 2-DG after 48 hours. The data after 24 hours show no real change in LDH activity, whereas the 2-DG-treatment for 48 hours at least results in a slight increase in LDH activity up to 116 % at 25 mM 2-DG.

## Resazurin reduction

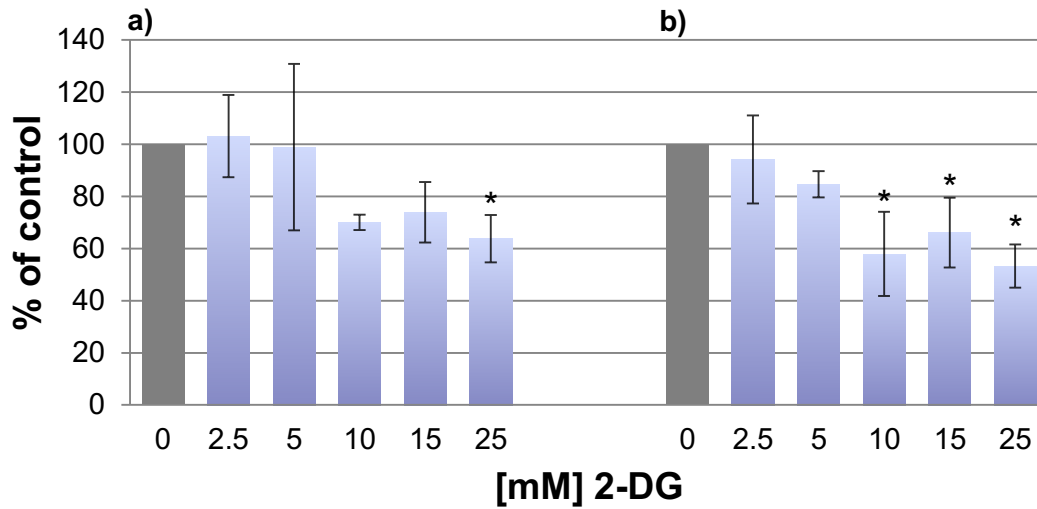


**Figure 18. Resazurin reduction in N18TG2 neuroblastoma after exposure to 2-DG for (a) 24 hours and (b) 48 hours.** Data are expressed as means  $\pm$  SD of 4 independent experiments.  $P < 0.05$  (\*) determined with Kruskal-Wallis (H)-test followed by Chi<sup>2</sup>-test.

The capacity of reducing resazurin of neuroblastoma cells decreases after treatment with 2-DG for 24 and 48 hours. 2.5 mM and 5 mM 2-DG did not seem to affect the cells after 24 hours, whereas the higher concentrations reveal to have an effect on cellular metabolism. Interestingly, from 10 mM onwards, capacity of reducing resazurin nearly remained the same after 24 and 48 hours.

## Protein content

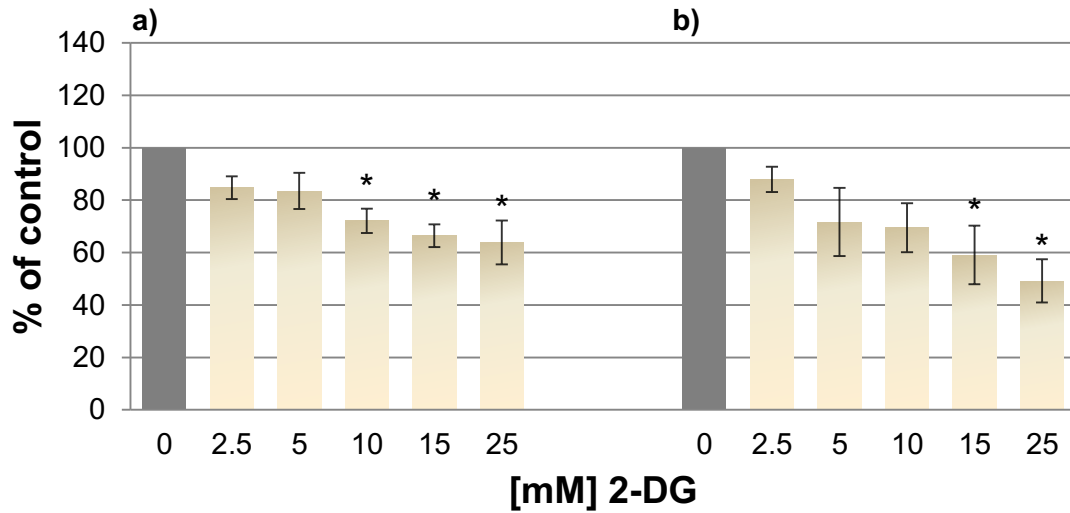


**Figure 19. Protein content in N18TG2 neuroblastoma after exposure to 2-DG for (a) 24 hours and (b) 48 hours.** Data are expressed as means  $\pm$  SD of 4 independent experiments.  $P < 0.05$  (\*) determined with Kruskal-Wallis (H)-test followed by Chi<sup>2</sup>-test.

A continuous decrease in protein content of neuroblastoma cells can be seen after treatment with 2-DG for 24 and 48 hours. From 10 mM onwards, protein content nearly remained the same after 24 hours, whereas these concentrations led to a modest diminishment in protein content after 48 hours.

### 3.1.3. Comparison between metabolism of glioma and neuroblastoma upon treatment with 2-deoxy-D-glucose

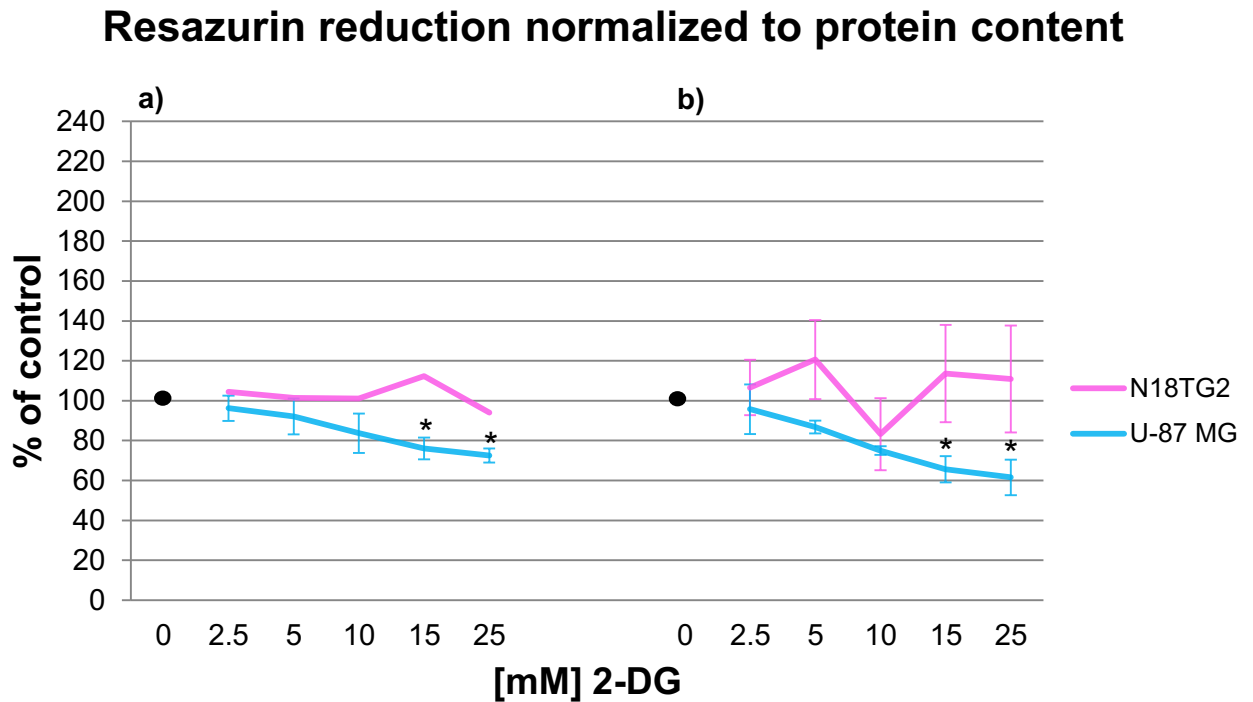


**Figure 20.** Comparison between N18TG2 neuroblastoma and U-87 MG glioma regarding resazurin reduction normalized to protein content after exposure to 2-DG for (a) 24 hours and (b) 48 hours. Data are expressed as means  $\pm$  SD of 4 independent experiments.  $P < 0.05$  (\*) determined with Kruskal-Wallis (H)-test followed by Chi<sup>2</sup>-test.

A reduction in capacity of resazurin formation can be observed in U-87 MG glioma cells after 24 and 48 hours in high concentrations of 2-DG, whereas in neuroblastoma cells no significant change in overall metabolism could be detected.

Since 10 mM 2-DG revealed to inhibit overall cellular metabolism by approximately 25 %, this concentration was used for all subsequent experiments.

## 3.2. Cannabidiol in glioma and neuroblastoma cells

### 3.2.1. Cannabidiol in glioma

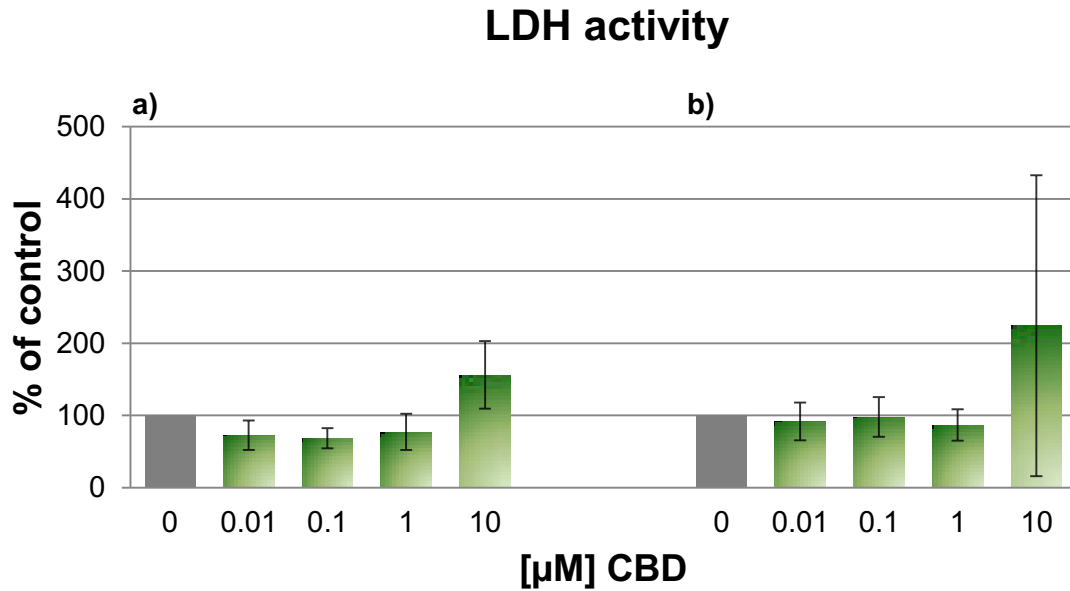


**Figure 21. LDH activity in U-87 MG glioma after exposure to CBD for (a) 24 hours and (b) 48 hours.** Data are expressed as means  $\pm$  SD of 4 independent experiments. Statistical evaluation does not reveal any significant changes.

0.01 – 1  $\mu$ M CBD nearly did not affect the glioma cells after 24 and 48 hours. 10  $\mu$ M CBD revealed to be the first concentration to exhibit a rise in LDH activity, indicating the cytotoxic effects of CBD.

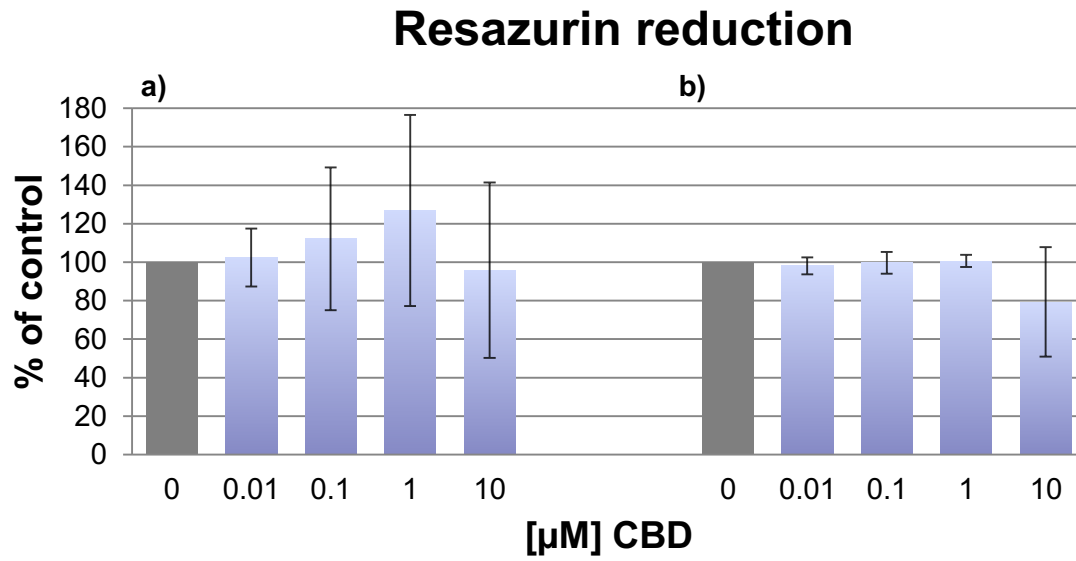


**Figure 22. Resazurin reduction in U-87 MG glioma after exposure to CBD for (a) 24 hours and (b) 48 hours.** Data are expressed as means  $\pm$  SD of 4 independent experiments. Statistical evaluation does not reveal any significant changes.

Although the data of the capacity of reducing resazurin in glioma cells do not show significant changes, a trend can be seen in cultures of 48 hours CBD-treatment at a concentration of 10  $\mu$ M. Still, 10  $\mu$ M CBD revealed to diminish overall cellular metabolism by 5 % after 24 hours and by 20 % after 48 hours, albeit not significant.

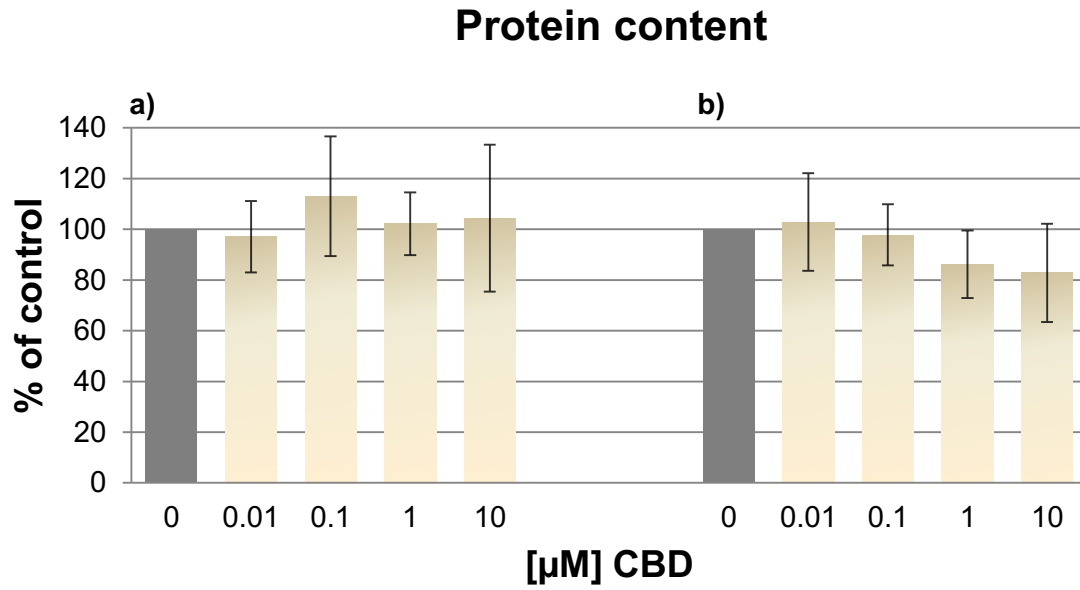


**Figure 23. Protein content in U-87 MG glioma after exposure to CBD for (a) 24 hours and (b) 48 hours.** Data are expressed as means  $\pm$  SD of 4 independent experiments. Statistical evaluation does not reveal any significant changes.

The data of protein content of glioma cells reveal no significant differences in all conditions, but a trend is displayed after 48 hours, whereat 1  $\mu$ M and 10  $\mu$ M CBD reduce protein content.

### 3.2.2. Cannabidiol in neuroblastoma

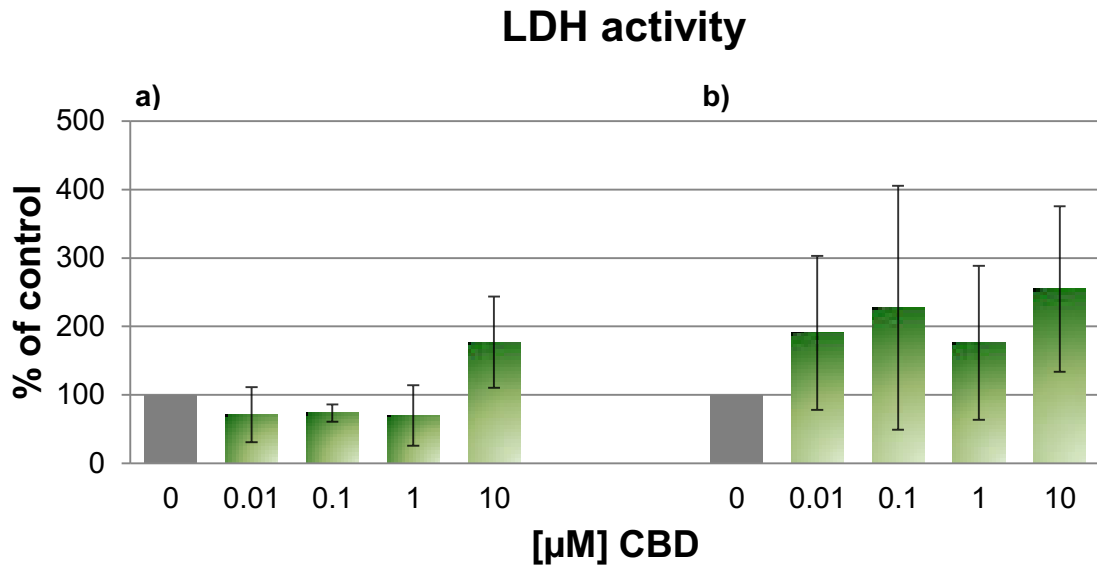


**Figure 24.** LDH activity in N18TG2 neuroblastoma after exposure to CBD for (a) 24 hours and (b) 48 hours. Data are expressed as means  $\pm$  SD of 4 independent experiments. Statistical evaluation does not reveal any significant changes.

Measurements of LDH activity in neuroblastoma do not result in significant changes, but nevertheless reveal a trend that can be seen clearly after 24 hours. 10  $\mu$ M CBD increased LDH activity by 77 % after 24 hours. Increase in LDH activity at 10  $\mu$ M CBD goes up to 255 % after 48 hours.

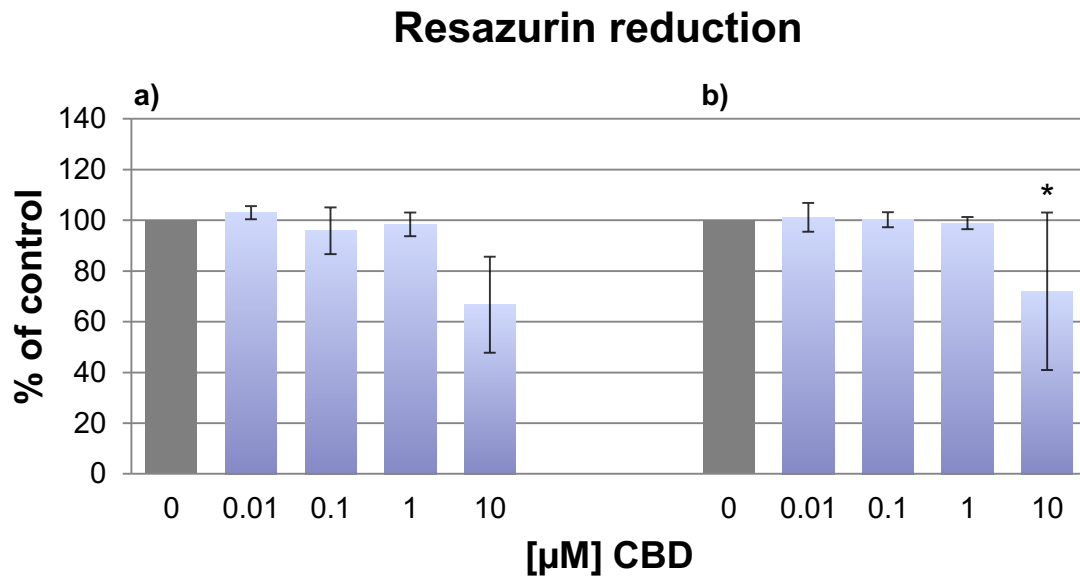


**Figure 25. Resazurin reduction in N18TG2 neuroblastoma after exposure to CBD for (a) 24 hours and (b) 48 hours.** Data are expressed as means  $\pm$  SD of 4 independent experiments.  $P < 0.05$  (\*) determined with Kruskal-Wallis (H)-test followed by  $\text{Chi}^2$ -test.

A clear trend of overall cell metabolism in neuroblastoma cells can be seen after 24 and 48 hours, although significance can only be seen at 10  $\mu\text{M}$  CBD after 48 hours.

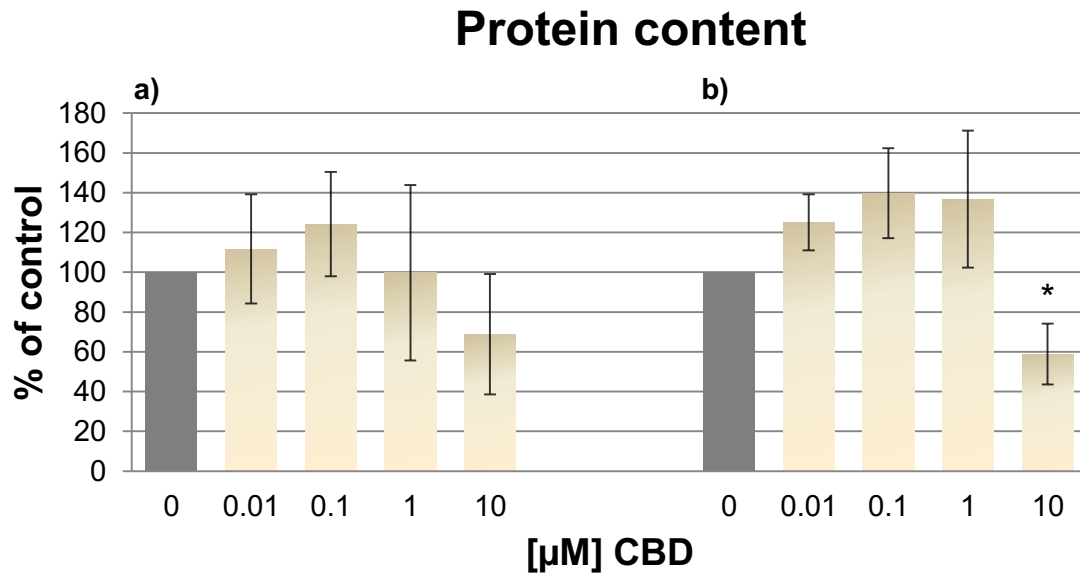


**Figure 26. Protein content in N18TG2 neuroblastoma after exposure to CBD for (a) 24 hours and (b) 48 hours.** Data are expressed as means  $\pm$  SD of 4 independent experiments.  $P < 0.05$  (\*) determined with Kruskal-Wallis (H)-test followed by Chi<sup>2</sup>-test.

Although data of protein content in neuroblastoma cells show high SDs, a loss of protein content can be seen at 10  $\mu$ M CBD after 24 and 48 hours with significance for the latter one.

### 3.2.3. Comparison between metabolism of glioma and neuroblastoma upon treatment with cannabidiol

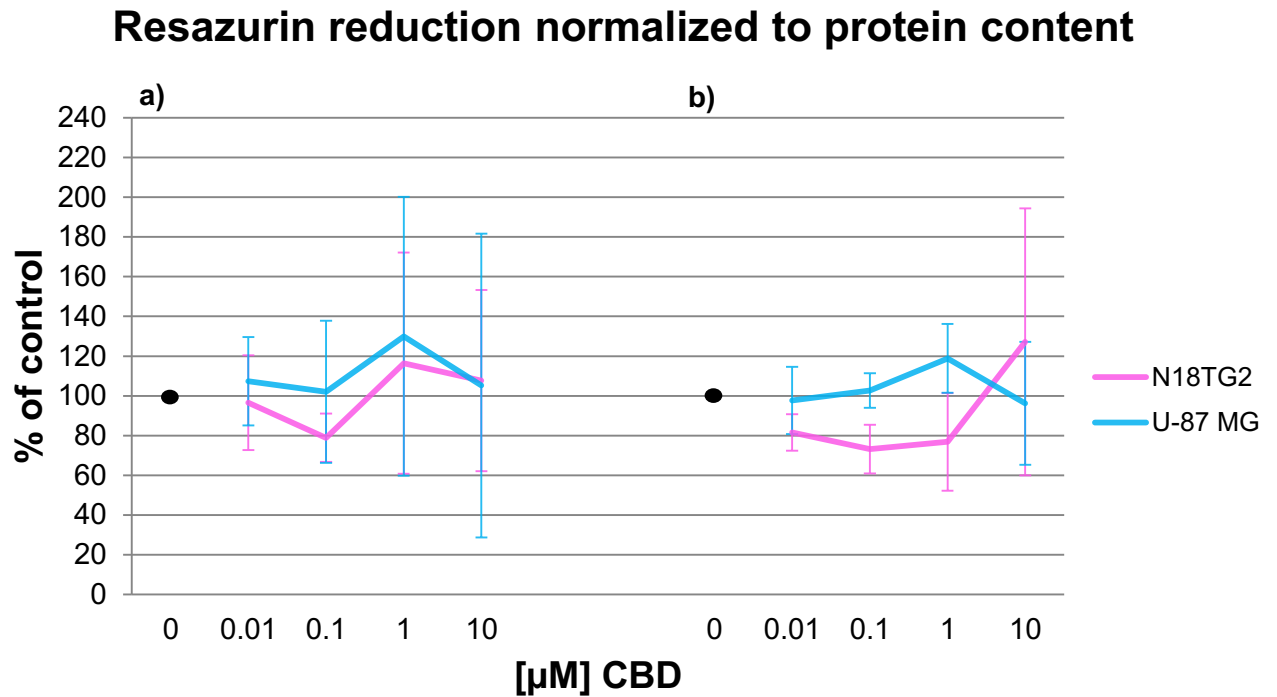


**Figure 27. Comparison between N18TG2 neuroblastoma and U-87 MG glioma regarding resazurin reduction normalized to protein content after exposure to CBD for (a) 24 hours and (b) 48 hours.** Data are expressed as means  $\pm$  SD of 4 independent experiments. Statistical evaluation does not reveal any significant changes.

The data for both cell line types is very volatile. However, it can be seen that 10  $\mu$ M CBD led to a capacity of reducing resazurin in glioma cells of 105 % and 96 % after 24 and 48 hours, respectively, and 107 % and 127 % in neuroblastoma cells after 24 and 48 hours.

### 3.3. Cannabidiol and 2-deoxy-D-glucose in glioma and neuroblastoma cells

#### 3.3.1. Cannabidiol and 2-deoxy-D-glucose in glioma

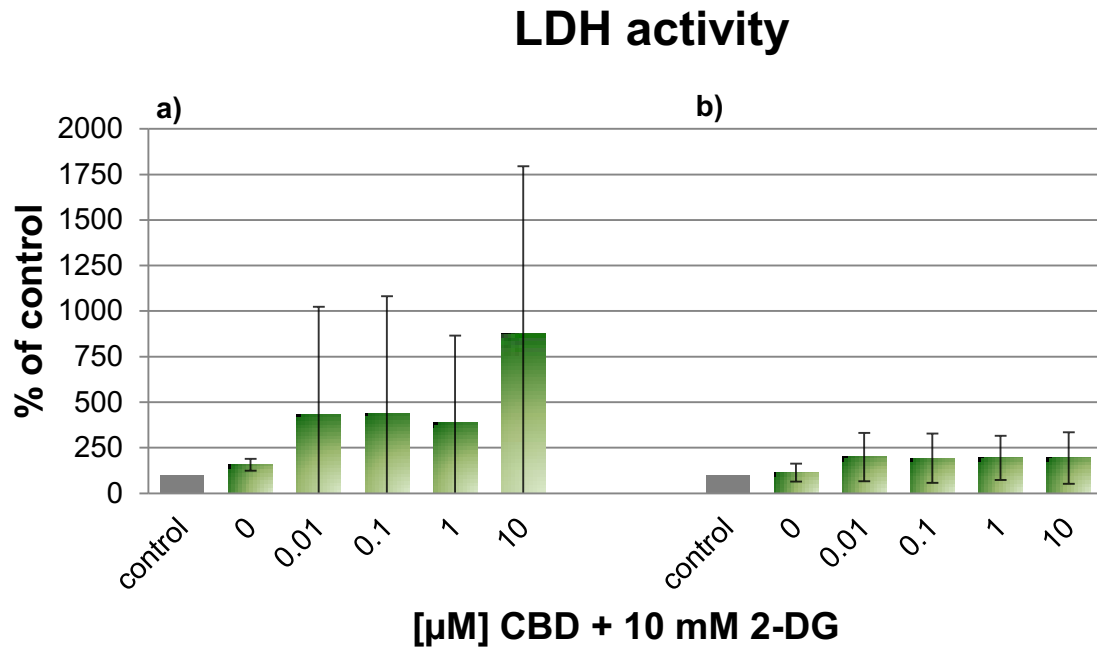


**Figure 28.** LDH activity in U-87 MG glioma after exposure to CBD and 10 mM 2-DG for (a) 24 hours and (b) 48 hours. Data are expressed as means  $\pm$  SD of 4 independent experiments. Statistical evaluation does not reveal any significant changes.

An ample increase in LDH activity of glioma cells occurs after treatment with CBD and 2-DG for 24 hours with enhancing LDH activity up to 878 % at 10  $\mu$ M CBD and 10 mM 2-DG. Nonetheless, due to the high SDs, this increase is not significant.

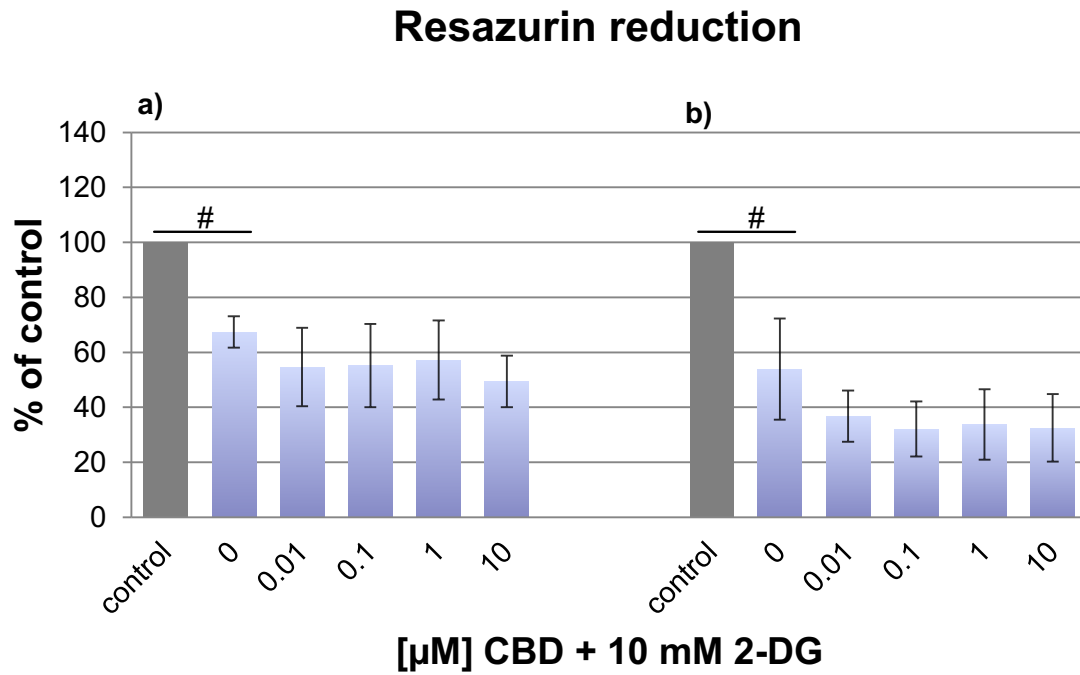


**Figure 29. Resazurin reduction in U-87 MG glioma after exposure to CBD and 10 mM 2-DG for (a) 24 hours and (b) 48 hours.** Data are expressed as means  $\pm$  SD of 4 independent experiments.  $P < 0.05$  (#) determined with Mann-Whitney-U-test for comparison between the control group and the group that was treated with 2-DG.

Capacity of reducing resazurin in glioma cells displays a clear trend. Although not significant, a further decrease in resazurin reduction can be seen after concomitant treatment with CBD and 2-DG by approximately 10 % after 24 hours and approximately 20 % after 48 hours in comparison to treatment with 2-DG alone.

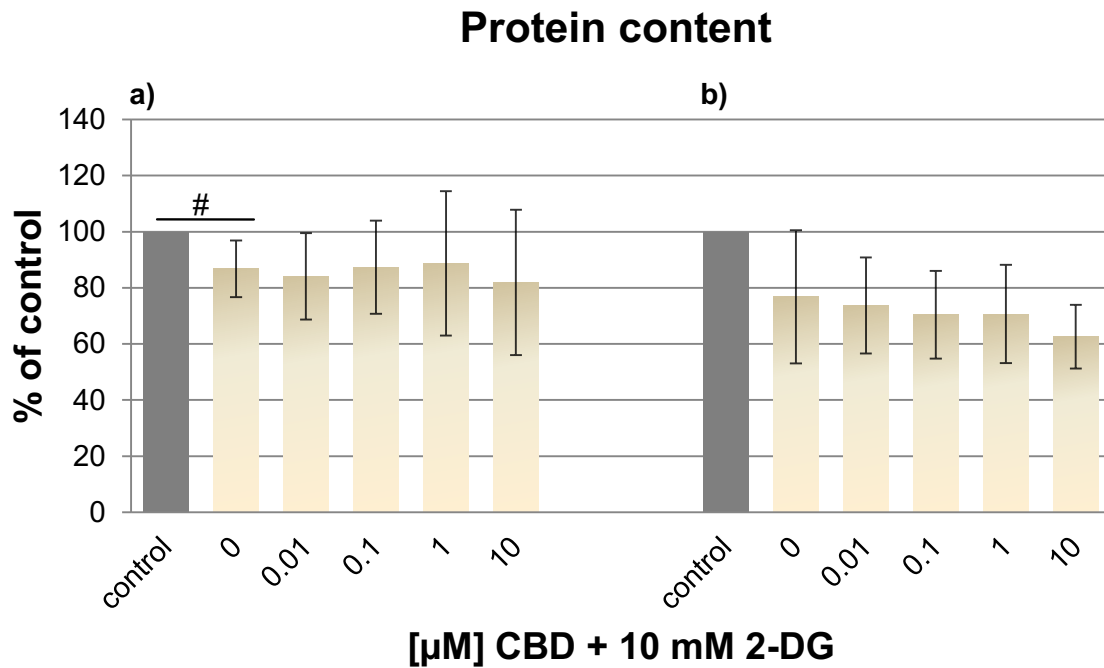


**Figure 30. Protein content in U-87 MG glioma after exposure to CBD and 10 mM 2-DG for (a) 24 hours and (b) 48 hours.** Data are expressed as means  $\pm$  SD of 4 independent experiments.  $P < 0.05$  (#) determined with Mann-Whitney-U-test for comparison between the control group and the group that was treated with 2-DG.

Protein content of glioma cells nearly remains the same after concomitant treatment with 2-DG and CBD after 24 and 48 hours. Protein content of 10 mM 2-DG is decreased by 14 %, whereas protein content of 10 mM 2-DG and 10  $\mu$ M CBD is reduced by 19 % after 24 hours. After 48 hours, protein content of 10 mM 2-DG is decreased by 24 %, whereas protein content of 10 mM 2-DG and 10  $\mu$ M CBD is lowered by 38 %.

### 3.3.2. Cannabidiol and 2-deoxy-D-glucose in neuroblastoma

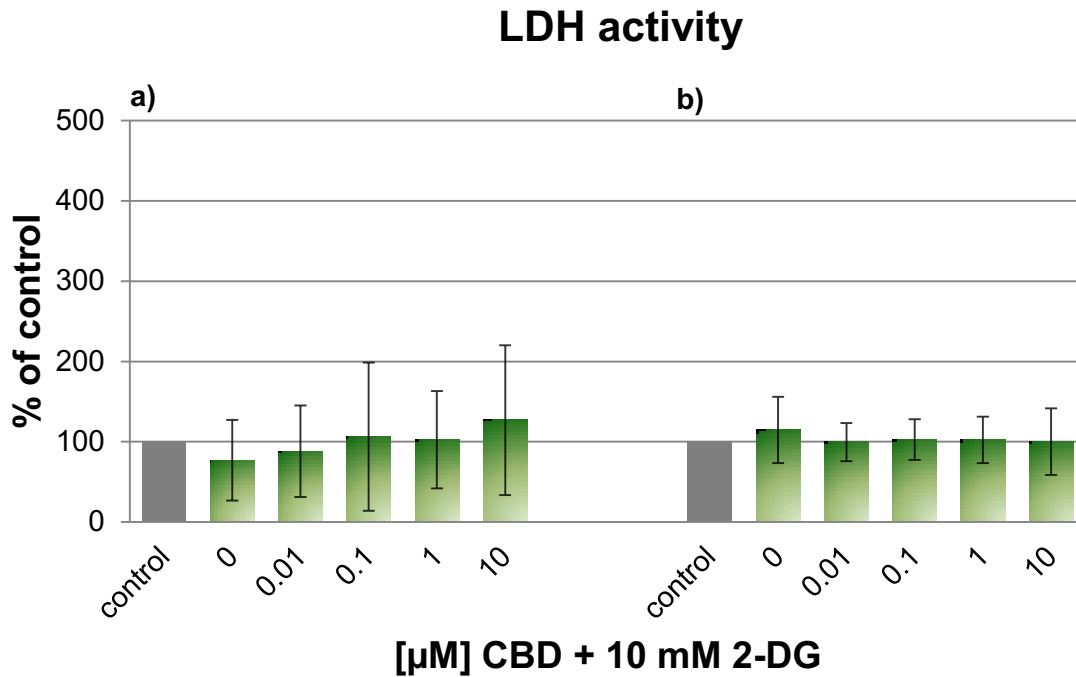


**Figure 31. LDH activity in N18TG2 neuroblastoma after exposure to CBD and 10 mM 2-DG for (a) 24 hours and (b) 48 hours.** Data are expressed as means  $\pm$  SD of 6 independent experiments. Statistical evaluation does not reveal any significant changes.

It can be seen that the concomitant treatment of CBD and 2-DG did not affect the cells after 24 and 48 hours significantly. Also no trend to an increase or decrease of cell degeneration can be observed.

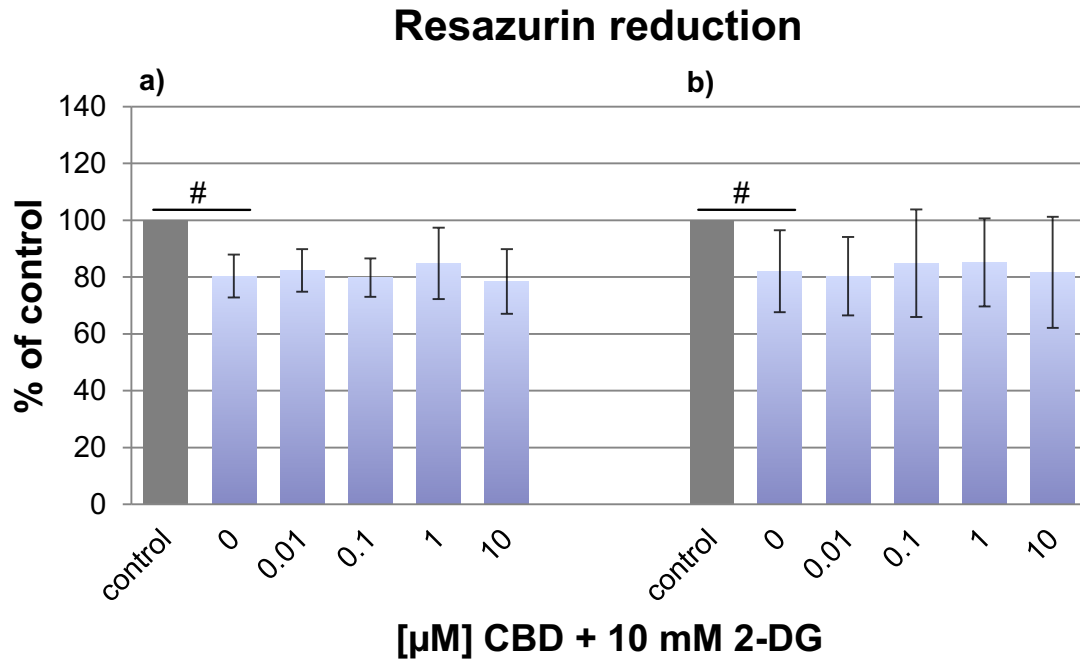


**Figure 32. Resazurin reduction in N18TG2 neuroblastoma after exposure to CBD and 10 mM 2-DG for (a) 24 hours and (b) 48 hours.** Data are expressed as means  $\pm$  SD of 6 independent experiments.  $P < 0.05$  (#) determined with Kruskal Mann-Whitney-U-test for comparison between the control group and the group that was treated with 2-DG.

A clear trend in capacity of reducing resazurin in neuroblastoma cells can be seen after 24 and 48 hours, whereas values range from 78 - 84 % resazurin conversion for both data.

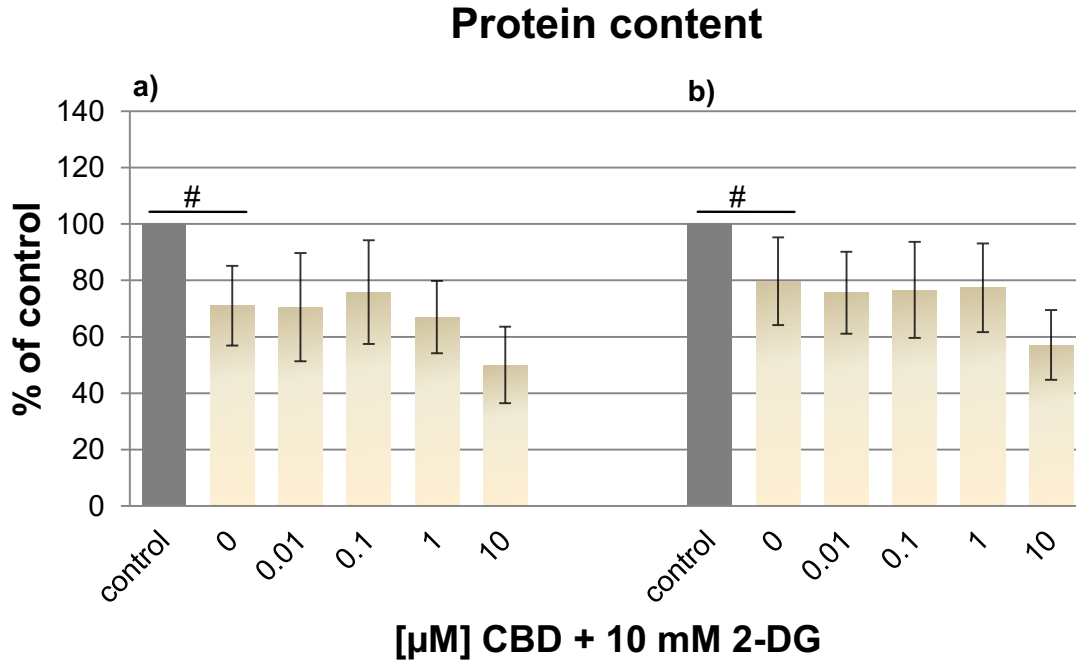


**Figure 33. Protein content in N18TG2 neuroblastoma after exposure to CBD and 10 mM 2-DG for (a) 24 hours and (b) 48 hours.** Data are expressed as means  $\pm$  SD of 6 independent experiments.  $P < 0.05$  (#) determined with Mann-Whitney-U-test for comparison between the control group and the group that was treated with 2-DG.

Although no significance is displayed, a trend is seen. Protein content of neuroblastoma cells nearly remains the same for treatment with 10 mM 2-DG alone and treatment with 10 mM 2-DG and 0.01 – 1  $\mu$ M CBD. Only 10 mM 2-DG and 10  $\mu$ M CBD decrease protein content of neuroblastoma cells to 50 % after 24 hours and 57 % after 48 hours.

### 3.3.3. Comparison between metabolism of glioma and neuroblastoma upon treatment with cannabidiol and 2-deoxy-D-glucose

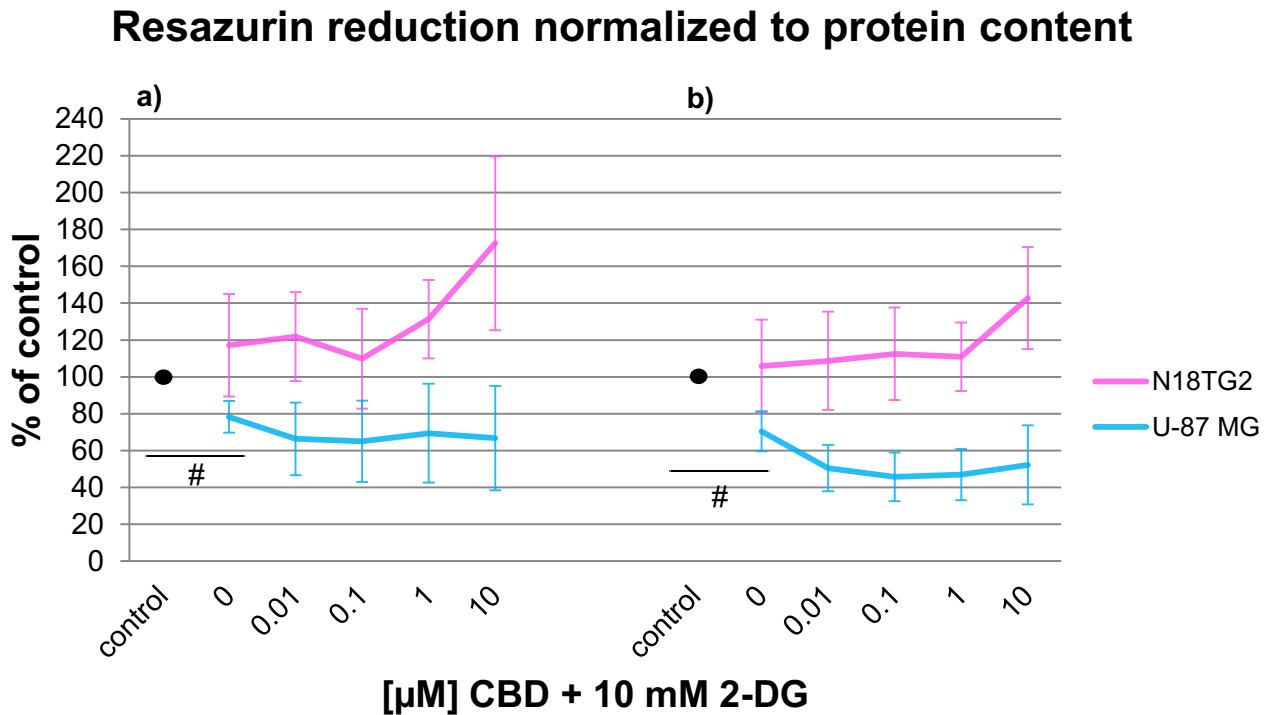


**Figure 34. Comparison between N18TG2 neuroblastoma and U-87 MG glioma regarding resazurin reduction normalized to protein content after exposure to CBD and 10 mM 2-DG for (a) 24 hours and (b) 48 hours.** Data are expressed as means  $\pm$  SD of 6 independent experiments with N18TG2 neuroblastoma cells and 4 independent experiments with U-87 MG glioma cells.  $P < 0.05$  (#) determined with Mann-Whitney-U-test for comparison between the control group and the group that was treated with 2-DG.

A continuous decrease in resazurin reduction capacity of glioma cells was revealed after 24 and 48 hours. Resazurin reduction in neuroblastoma cells increased slightly after 24 and 48 hours.

### 3.4. 2-deoxy-D-glucose in murine mesencephalic primary cells

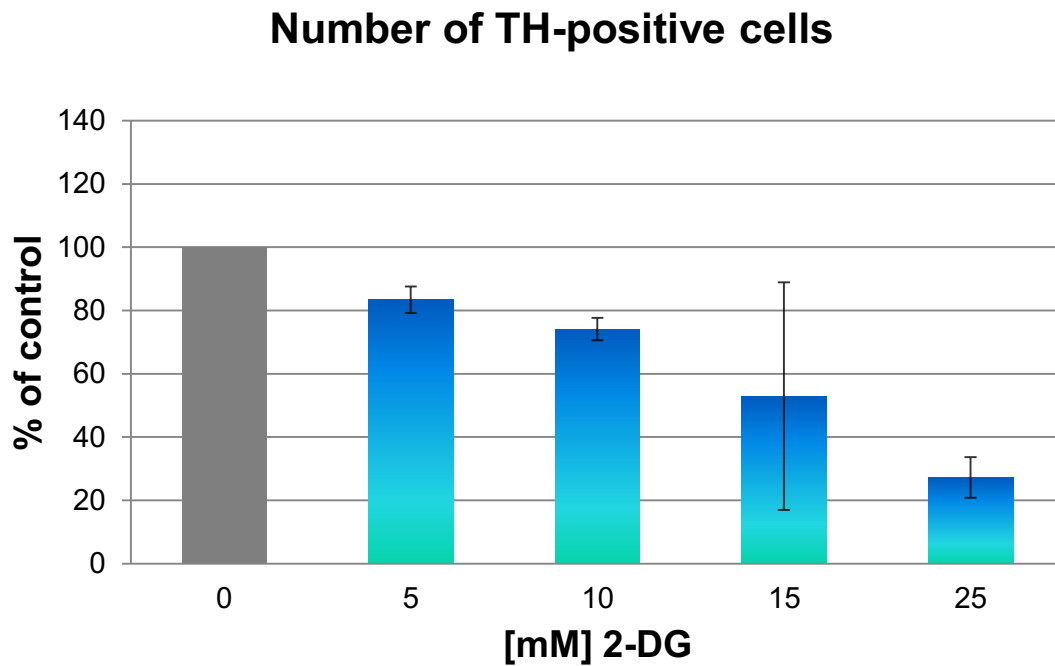


**Figure 35. Number of TH-positive murine primary cells after exposure to 2-DG.** Data are expressed as means  $\pm$  SD of 1 experiment. Statistical evaluation cannot be compiled.

A steady decrease in the number of dopaminergic neurons can be seen after treatment with 2-DG. The highest concentration of 2-DG reduced the amount of these cells to 27 %.

## 4. Discussion

### 4.1. General remarks

It can be seen clearly that the measurement of LDH activity is often very volatile and especially the measurement of LDH activity in glioma cells upon concomitant treatment of CBD and 2-DG displays enormous high values (Figure 28). Since access to the laboratory had been restricted due to SARS-CoV-2 pandemic, time was missing for troubleshooting of this method. Thus, the measurement of LDH activity within this study cannot be considered a reliable indicator for cell viability.

### 4.2. 2-deoxy-D-glucose in glioma and neuroblastoma cells

Since 2-DG acts as a competitive inhibitor of glycolysis, we chose to use this substance in order to reduce glycolysis in our following experiments. We hypothesized that the toxic effect of CBD would be augmented by the simultaneous treatment with 2-DG. Thus, we sought a 2-DG-concentration that diminishes overall cell viability by only 25 %.

Several other studies revealed that it clearly depends on the cell type which concentration of 2-DG leads to a decrease in cell viability by 25 %. 10 mM 2-DG have shown to diminish cell proliferation of SK-N-AS neuroblastoma cells by 40 %, whereas the same concentration leads to a decrease in cell proliferation by 80 % in IMR-32 neuroblastoma after 24 hours (Chuang et al. 2013).

Thus, it can be concluded that the appropriate concentration of 2-DG must be tested specifically for each cell line type. In this study, 10 mM revealed to be an appropriate concentration for our cells.

After 4 independent experiments it can be seen that our cell lines reacted differently to the partial inhibition of glycolysis by 2-DG.

The LDH activity of both cell lines varies strongly between experiments, especially at 24 hours (Figure 14, a and 17, a), but a slight increase in LDH activity can be seen in neuroblastoma cells after 48 hours (Figure 17, b). Surprisingly, a decrease in LDH activity of glioma cells can be registered after 48 hours (Figure 14, b) at the highest two concentrations of 2-DG. Nevertheless, the data are very scattered and therefore cannot be considered a reliable indicator for cell viability.

The capacity of reducing resazurin decreases continuously in both cell lines and is very similar to each other at the highest concentrations of 2-DG after 24 and 48 hours, whereby resazurin reduction is reduced to 60 % and 50 %, respectively (Figure 15 and 18). However, the two lowest concentrations of 2-DG, 2.5 mM and 5 mM, affect glioma cells but don't alter capacity of reducing resazurin in neuroblastoma cells after 24 hours. This indicates that the metabolism of glioma cells is affected faster than the metabolism of neuroblastoma cells. Regarding the protein content, a continuous decrease can be seen for both cell lines (Figure 16 and 19), although the amount of protein remained relatively stable in glioma cells at 10 – 25 mM 2-DG after 24 and 48 hours. But, if one consider the capacity of reducing resazurin normalized to the protein content, a continuous decrease can be identified in glioma cells, but not in neuroblastoma cells, where percental resazurin reduction remained the same throughout all tested concentrations of 2-DG (Figure 20). This implicates that some glioma cells die and the metabolic activity of the surviving cells decreases, while some neuroblastoma cells die and the metabolic activity of the surviving cells remains the same.

Thus, it can be inferred from our data that both, glioma and neuroblastoma, suffer from partial inhibition of glycolysis and subsequently die, but the glioma cells react more sensitively to loss of glycolytic capacity than the neuroblastoma cells do.

Neurons and glial cells have already been described to consume glucose to a high extent. But, the way how these two cell types metabolise glucose is different. Glial cells depend more on glycolysis, whereas neurons obtain their energy from oxidative phosphorylation, which could be proven in primary cell culture (Magistretti and Allaman 2015). Neurons produce more CO<sub>2</sub> than astrocytes do, which indicates an enhanced CAC. Additionally, astrocytes contain more phosphorylated PDH than neurons do. Since the conversion of pyruvate into acetyl-CoA is a highly regulated process, in which phosphorylation of PDH decreases its activity and thus, diminishes production of acetyl-CoA, a higher content of phosphorylated PDH in astrocytes indicates that these cells rely more on glycolysis than they do on CAC and oxidative phosphorylation (Magistretti and Allaman 2015). The enhanced glycolytic activity is triggered through glutamate uptake and leads to an enhanced production of lactate which is transferred to neurons. The neurons convert the lactate to pyruvate and subsequently, incorporate it into the CAC. Additionally, glutamate is converted to glutamine in astrocytes and is subsequently transferred to the neurons in order to serve as a supplying substrate for the CAC and to recycle glutamate. This mechanism of astrocytes providing energy in the form of lactate to the neurons upon glutamate uptake is called "astrocyte-to-neuron lactate shuttle" (ANLS) (Magistretti and Allaman 2015; Mergenthaler et al. 2013).

The ANLS remains a controversial topic to date. Neurons express the glucose transporter 3, which allows a direct import of glucose into the cells. Next, the ANLS could not be proven in stimulated neurons because it resulted in an enhanced glycolysis within neurons but not in an enhanced lactate uptake.

But the LDH-isoform 5, that converts pyruvate into lactate, is abundantly expressed in astrocytes, whereas the LDH-isoform 1, that converts lactate into pyruvate, is primarily expressed in neurons (Jha and Morrison 2018), which further indicates the existence of ANLS. This corresponds to our findings since the glioma cells reacted more sensitively to glucose deprivation, which can be seen in the capacity of resazurin reduction normalized to the protein content after 24 and 48 hours (Figure 20). The metabolic activity in these cells continuously decreases, yielding in significant results at 15 mM and 25 mM after 24 and 48 hours, whereas the metabolic activity of neuroblastoma cells remains the same throughout the whole experiment (Figure 20). This further implicates that the diminishment of glycolysis does more harm to glioma cells than to neuroblastoma cells, which can be explained by the dependence of glial cells on glycolysis.

Nonetheless, it has to be mentioned that glioma and neuroblastoma cells are cancer cells and thus, differ greatly from healthy glial cells and neurons. It is known that cancer cells depend largely on glycolysis rather than oxidative phosphorylation. From this point of view, our data is contradictory because the diminishment of glycolysis must have ultimately led to a similarly decreased cellular metabolism in both cell types, which is not the case in this study.

### **4.3. Cannabidiol in glioma and neuroblastoma cells**

Although not so many significant differences could be statistically verified, CBD seems to affect the glioma and neuroblastoma cells similarly. 10  $\mu$ M CBD diminishes resazurin reduction capacity and protein content in glioma and neuroblastoma cells to nearly the same extent (Figure 22, 23, 25 and 26), except the protein content in glioma cells after 24 hours (Figure 23, a). Regarding the capacity of reducing resazurin normalized to the protein content (Figure 27), it can be found that glioma and neuroblastoma cells did not experience a reduction of the overall metabolic activity in CBD-treated cultures. The cells rather die and if they survive, their metabolism is not altered.

This is in accordance to recent findings of the cytotoxicity of CBD. 10  $\mu$ M CBD has already been revealed to exert toxic effects to N18TG2 neuroblastoma cells. Mitochondrial respiratory chain has been reduced to 60 % of control levels (Unterberger 2016). All complexes of the electron transport chain are affected by CBD, in which complex I is the

most affected of all (Singh et al. 2015). Thus, it can be concluded that CBD inhibits oxidative phosphorylation and forces the cells to shift to another energy-generating pathway.

The fact that CBD decreased cellular metabolism similarly in both cell types corresponds partly to the above described findings. Since the main energy-generating pathway in cancer cells is glycolysis and CBD is known to affect mitochondrial respiratory chain, it is reasonable that CBD diminished cellular metabolism in both cancer cell types. But since our cells displayed glial-cell-like and neuron-like response to the partial inhibition of glycolysis by 2-DG, it is not obvious why CBD affected both cell types similarly. It was expected that CBD affects the neuroblastoma cells more than the glioma cells, which is not the case in this study.

#### **4.4. Cannabidiol and 2-deoxy-D-glucose in glioma and neuroblastoma cells**

This study is the first one to investigate the toxic effects of CBD upon inhibition of glycolysis by 2-DG in cancer cells. Since CBD is known to inhibit mitochondrial respiratory chain, this might be one reason how CBD exerts its anticarcinogenic effects (Singh et al. 2015; Unterberger 2016). Thus, the additional partial inhibition of glycolysis is likely to ultimately leading to enhanced cell death.

Interestingly, our data depict the opposite. The partial inhibition of glycolysis in combination with CBD did not augment the toxic effects of CBD. Since cancer cells obtain their energy mainly from glycolysis, it is probable that our cancer cells generated their energy from another source.

Cells can normally use the non-essential amino acid glutamine in order to produce amino acids and nucleotides as well as energy. It is taken up by the cells, subsequently forms glutamate by the action of glutaminase and is finally converted into  $\alpha$ -ketoglutarate by glutamate dehydrogenase, which is incorporated into the CAC. Due to the excessive growth of tumours, they compensate their loss of essential intermediates of the CAC by enhanced uptake of glutamine. Especially citrate is used by cancer cells in order to produce fatty acids and cholesterol for cell proliferation. Furthermore, glutamine provides nitrogen for production of purines and pyrimidines and contributes to the production of non-essential amino acids. In addition, energy is produced through coupling oxidative phosphorylation to glutamine-driven CAC (Chen and Cui 2015; Gonzalez Herrera et al. 2015). It has already been reported that especially glioma consume a vast amount of glutamine that definitely exceeds their glutamine demand for protein and nucleotide biosynthesis (DeBerardinis et al. 2007).

The treatment with CBD alone leads to a partial inhibition of mitochondrial respiratory chain but it does not affect cell survival in neuroblastoma cells. It rather puts the cells into a quiescent state (Unterberger 2016). Therefore, glycolysis and oxidative phosphorylation, the major energy-generating sources of the cells, were partially inhibited and still the cells managed to overcome these damaging events. Since our media contained L-glutamine, it is likely that the glioma and neuroblastoma cells are able to implement the use of glutaminolysis for ATP-formation when glycolysis and oxidative phosphorylation were inhibited by 2-DG and CBD in order to fulfil their energy demand.

Interestingly, the response of the glioma and neuroblastoma cells to treatment with CBD in combination with 2-DG differ to a high extent. Although not significant, it can be seen that the co-treatment of CBD with 2-DG diminishes overall cellular metabolism in glioma by 20 % in comparison to the treatment with 2-DG alone after 24 and 48 hours (Figure 29). In contrast, the combination of CBD and 2-DG in neuroblastoma did not alter the overall cellular metabolism in comparison to the treatment with 2-DG alone (Figure 32). This is in accordance to the above described effects of 2-DG-treatment within these cells. This experiment revealed a clear diminishment in metabolic activity of glioma cells, but not in neuroblastoma cells which again can be observed when these cells are treated with CBD in combination with 2-DG. This leads to a conflict, since the less sensitivity of neuroblastoma cells to a 2-DG treatment can be explained by the enhanced dependence of neurons on oxidative phosphorylation, but neuroblastoma and glioma are both cancer cells and therefore, glycolysis should be their main energy-generating pathway.

A clear explanation of why the neuroblastoma cells show a less sensitivity to partial inhibition of glycolysis by 2-DG than glioma cells do, cannot be made regarding our data. Furthermore, it needs to be stated that the cancer cells within an individual definitely differ from cancer cell lines in culture (Vogel et al. 2005), since the environment within a living organism is not exactly the same as the environment within cell culture. Therefore, cancer cells within a living organism, cell lines and primary neurons and glia cells can be seen as quite different systems and an explanation of why the neuroblastoma cells reacted that insensitively to partial inhibition of glycolysis by 2-DG and the concomitant treatment of CBD and 2-DG cannot be made without running the risk of becoming speculative.

#### **4.5. 2-deoxy-D-glucose in murine mesencephalic primary cells**

Due to Sars-CoV-2 pandemic, only one experiment with 2-DG could be conducted with the murine mesencephalic primary cells (Figure 35). Although no statistics can be compiled, it can be seen that 2-DG seems to reduce the amount of TH-positive cells steadily.

## 5. Conclusion

Due to Sars-CoV-2 pandemic, experiments with primary cell culture could not be conducted.

(1) Which concentration of 2-DG decreases overall cellular viability by 25 % in primary neural cells and cancer cells?

10 mM 2-DG reveals to be an appropriate concentration for the partial inhibition of glycolysis for the U-87 MG glioma and N18TG2 neuroblastoma cells.

(2) Which concentration of CBD acts cytotoxicly to primary neural cells and cancer cells?

10  $\mu$ M CBD act similarly cytotoxic to U-87 MG glioma and N18TG2 neuroblastoma cells.

(3) Does the inhibition of glycolysis by 2-DG augment the toxic effect of CBD in primary neural cells and cancer cells?

No, the simultaneous partial inhibition of glycolysis by 2-DG within U-87 MG glioma and N18TG2 neuroblastoma cells did not augment the cytotoxic effects of CBD. Although not significant, a slight diminishing tendency can be seen in U-87 MG glioma cells. Since this cell type depends more on glycolysis than the neuroblastoma cells do, it is reasonable that they suffer more from partial inhibition of glycolysis.

Further investigation is necessary. It is likely that the glioma and neuroblastoma cells utilised glutamine in order to fulfil their energy demand. Therefore, experiments with a glutamine-low and even pyruvate-low medium are proposed.

(4) Do the neuroblastoma and glioma cells react similarly to the treatment with 2-DG, CBD and CBD in combination with 2-DG?

The U-87 MG glioma and N18TG2 neuroblastoma cells reacted nearly similarly to the treatment with CBD, but the response to the treatment with 2-DG alone and the concomitant treatment with CBD and 2-DG differ to a high extent. Glial cells depend more on glycolysis than neurons do and this could explain why treatment with 2-DG and the simultaneous treatment of CBD and 2-DG exert different effects in these cell types.

## 6. Summary

### 6.1. English

CBD, a constituent of the plant *Cannabis sativa*, has been described to exert a plethora of therapeutical effects. Especially its effects on cancer cells are of notable interest since CBD has shown to exert anticarcinogenic effects. Anti-proliferative effects were shown in lung, breast and brain cancer as well as tumours of the hematopoietic and lymphoid tissues *in vivo* and *in vitro*. Since the treatment with CBD in brain cancer revealed to inhibit mitochondrial respiratory chain significantly without affecting cell survival in these, we hypothesized that concomitant inhibition of glycolysis, the main energy-generating pathway in cancer, would decrease cell viability to a high extent and would ultimately lead to enhanced cell death.

This study aimed to test, which concentration of CBD exerts anti-proliferative effects in glioma and neuroblastoma cells, if CBD-induced toxicity can be increased by partial inhibition of glycolysis and to which extent the reactions of glioma and neuroblastoma cells to the treatment with CBD with and without partial inhibition of glycolysis differ from each other.

Therefore, cell viability was determined with measurement of LDH activity, which is an approved method of quantifying the amount of dead cells. When cells undergo necrosis or apoptosis, LDH is released into the surrounding fluid and the consumption of its metabolites can be measured. Overall cellular metabolism was determined with measurement of reduction of resazurin into resorufin by viable mitochondria. Quantification of surviving cells was conducted using BCA-Protein Assay.

Our study reveals that CBD exerts toxic effects at 10  $\mu$ M and the response to CBD-treatment is relatively similar in glioma and neuroblastoma cells. The cytotoxic effects of CBD cannot be augmented by concomitant partial inhibition of glycolysis by 10 mM 2-DG. Glioma cells react more sensitively to simultaneous treatment with CBD and 2-DG than the neuroblastoma cells do. The same difference is displayed after treatment with 2-DG alone. This comes along with previously made findings that glial cells depend more on glycolysis than neurons do and thus, an increased sensitivity to glucose deprivation stands to reason.

Next, a study in which the cytotoxic effects of CBD under deprivation of glutamine are tested is necessary. Since cancer cells are capable of metabolise glutamine to a high extent in order to fulfil all requirements for extensive cell proliferation, a combination of CBD and a glutamine-low medium is proposed.

## 6.2. German

CBD, eine Substanz aus der Pflanze *Cannabis sativa*, werden therapeutische Wirkungen in vielen verschiedenen Krankheiten nachgesagt. Besonders interessant sind die Auswirkungen auf Krebszellen. Das Wachstum und die Lebensfähigkeit jener konnte durch die Zugabe von CBD stark gehemmt werden. Dies wurde bereits in Tumoren der Lunge, der Brust, des Hirns und des Knochenmarks *in vivo* und *in vitro* nachgewiesen. Es konnte bereits gezeigt werden, dass die Behandlung von Hirntumoren mit CBD zu einer signifikanten Hemmung der mitochondrialen Atmungskette führt, ohne hierbei die Überlebensfähigkeit der Zellen zu beeinträchtigen. Daher haben wir die Hypothese aufgestellt, dass der toxische Effekt von CBD verstärkt werde, wenn zusätzlich die Glykolyse, der Hauptversorgungsweg in Krebszellen, gehemmt wird.

Die Forschungsziele dieser Studie waren die folgenden: Welche CBD-Konzentration führt zu erheblichen toxischen Effekten in Gliomzellen und Neuroblastomzellen? Kann die toxische Wirkung von CBD durch partielle Blockade der Glykolyse verstärkt werden? Unterscheidet sich die Reaktion von Gliomzellen und Neuroblastomzellen auf die Behandlung von CBD mit und ohne partielle Blockade der Glykolyse?

Um dies herauszufinden, wurde die Lebensfähigkeit der Zellen mittels Messung der LDH-Aktivität, eine anerkannte Methode, bestimmt. LDH wird in die umliegende Flüssigkeit freigesetzt, wenn Zellen sterben. Den Verbrauch der LDH-Metaboliten kann man messen. Um den Grad des geschädigten Metabolismus zu ermitteln, wurde die Reduktion von Resazurin zu Resorufin gemessen. Die Mitochondrien der metabolisch aktiven Zellen können Resazurin reduzieren und daher ist diese Methode ein verlässlicher Indikator hierfür. Um die überlebenden Zellen zu quantifizieren, wurde der BCA-Protein-Assay verwendet.

Aus unseren Daten lässt sich schließen, dass CBD toxische Effekte bei einer Konzentration von 10  $\mu\text{M}$  erzielt. Die Auswirkungen dieser Behandlung sind nahezu ident in Gliomzellen und Neuroblastomzellen. Die toxischen Effekte von CBD können nicht durch partielle Blockade der Glykolyse gehemmt werden. Jedoch reagieren Gliomzellen empfindlicher auf eine gleichzeitige Behandlung mit CBD und 2-DG als die Neuroblastomzellen. Dieselbe Reaktion lässt sich bei der 2-DG-Behandlung feststellen. Dies geht Hand in Hand mit zuvor durchgeführten Studien, die eine höhere glykolytische Aktivität in Glia-Zellen als in Neuronen nachgewiesen haben.

Eine Studie, in der die Auswirkungen von CBD bei Entzug von Glutamin getestet werden, ist das nächste Ziel, da Krebszellen in der Lage sind weitaus mehr Glutamin als Energiequelle zu verwenden als gesunde Zellen.

## 7. References

- Abdel-Wahab, Ali F.; Mahmoud, Waheed; Al-Harizy, Randa M. (2019). Targeting glucose metabolism to suppress cancer progression: prospective of anti-glycolytic cancer therapy. *Pharmacological research*, 150:104511.
- Aghaee, Fahimeh; Pirayesh Islamian, Jalil; Baradaran, Behzaad (2012). Enhanced radiosensitivity and chemosensitivity of breast cancer cells by 2-deoxy-d-glucose in combination therapy. *Journal of breast cancer*, 15 (2):141–147.
- Allen, Marie; Bjerke, Mia; Edlund, Hanna; Nelander, Sven; Westermarck, Bengt (2016). Origin of the U87MG glioma cell line: Good news and bad news. *Science translational medicine*, 8 (354):354re3.
- Arias-Carrión, Oscar; Stamelou, Maria; Murillo-Rodríguez, Eric; Menéndez-González, Manuel; Pöppel, Ernst (2010). Dopaminergic reward system: a short integrative review. *International archives of medicine*, 3:24.
- Benard, Giovanni; Bellance, Nadège; Jose, Caroline; Rossignol, Rodrigue (2011). Relationships Between Mitochondrial Dynamics and Bioenergetics. In Bingwei Lu (Ed.): *Mitochondrial Dynamics and Neurodegeneration*. Dordrecht: Springer Netherlands:47–68.
- Bisogno, T. (2008). Endogenous cannabinoids: structure and metabolism. *Journal of neuroendocrinology*, 20 Suppl 1:1–9.
- Brusberg, Mikael; Arvidsson, Susanne; Kang, Daiwu; Larsson, Håkan; Lindström, Erik; Martinez, Vicente (2009). CB1 receptors mediate the analgesic effects of cannabinoids on colorectal distension-induced visceral pain in rodents. *The Journal of neuroscience : the official journal of the Society for Neuroscience*, 29 (5):1554–1564.
- Campbell, Mary K.; Farrel, Shawn O. (2006). *Biochemistry*. 5th ed. Australia: Thomson.
- Cell Lines Service. U-87 MG, [https://www.clsgmbh.de/p658\\_U-87\\_MG.html](https://www.clsgmbh.de/p658_U-87_MG.html), accessed on 01/05/2020.
- Cellosaurus. Cellosaurus cell line N18TG2 (CVCL\_2132), [https://web.expasy.org/cellosaurus/CVCL\\_2132](https://web.expasy.org/cellosaurus/CVCL_2132), accessed on 30/04/2020.

- Chen, Lian; Cui, Hengmin (2015). Targeting Glutamine Induces Apoptosis: A Cancer Therapy Approach. *International journal of molecular sciences*, 16 (9):22830–22855.
- Chuang, Jiin-Haur; Chou, Ming-Huei; Tai, Ming-Hong; Lin, Tsu-Kung; Liou, Chia-Wei; Chen, Tingya et al. (2013). 2-Deoxyglucose treatment complements the cisplatin- or BH3-only mimetic-induced suppression of neuroblastoma cell growth. *The international journal of biochemistry & cell biology*, 45 (5):944–951.
- Cifelli, Pierangelo; Ruffolo, Gabriele; Felice, Eleonora de; Alfano, Veronica; van Vliet, Erwin Alexander; Aronica, Eleonora; Palma, Eleonora (2020). Phytocannabinoids in Neurological Diseases: Could They Restore a Physiological GABAergic Transmission? *International journal of molecular sciences*, 21 (3).
- Creative Bioarray. Resazurin Cell Viability Assay, <https://www.creative-bioarray.com/support/resazurin-cell-viability-assay.htm>, accessed on 22/04/2020.
- DeBerardinis, Ralph J.; Mancuso, Anthony; Daikhin, Evgueni; Nissim, Ilana; Yudkoff, Marc; Wehrli, Suzanne; Thompson, Craig B. (2007). Beyond aerobic glycolysis: transformed cells can engage in glutamine metabolism that exceeds the requirement for protein and nucleotide synthesis. *Proceedings of the National Academy of Sciences of the United States of America*, 104 (49):19345–19350.
- Di Marzo, Vincenzo; Piscitelli, Fabiana (2015). The Endocannabinoid System and its Modulation by Phytocannabinoids. *Neurotherapeutics : the journal of the American Society for Experimental NeuroTherapeutics*, 12 (4):692–698.
- Filippis, Daniele de; Esposito, Giuseppe; Cirillo, Carla; Cipriano, Mariateresa; Winter, Benedicte Y. de; Scuderi, Caterina et al. (2011). Cannabidiol reduces intestinal inflammation through the control of neuroimmune axis. *PloS one*, 6 (12):e28159.
- Ganapathy-Kanniappan, Shanmugasundaram; Geschwind, Jean-Francois H. (2013). Tumor glycolysis as a target for cancer therapy: progress and prospects. *Molecular cancer*, 12:152.
- García-Arencibia, Moisés; González, Sara; Lago, Eva de; Ramos, José A.; Mechoulam, Raphael; Fernández-Ruiz, Javier (2007). Evaluation of the neuroprotective effect of cannabinoids in a rat model of Parkinson's disease: importance of antioxidant and cannabinoid receptor-independent properties. *Brain Research*, 1134 (1):162–170.

- Gomes, Felipe V.; Reis, Daniel G.; Alves, Fernando H. F.; Corrêa, Fernando M. A.; Guimarães, Francisco S.; Resstel, Leonardo B. M. (2012). Cannabidiol injected into the bed nucleus of the stria terminalis reduces the expression of contextual fear conditioning via 5-HT<sub>1A</sub> receptors. *Journal of psychopharmacology (Oxford, England)*, 26 (1):104–113.
- Gonzalez Herrera, Karina N.; Lee, Jaewon; Haigis, Marcia C. (2015). Intersections between mitochondrial sirtuin signaling and tumor cell metabolism. *Critical reviews in biochemistry and molecular biology*, 50 (3):242–255.
- Harry, G. J.; Billingsley, M.; Bruinink, A.; Campbell, I. L.; Classen, W.; Dorman, D. C. et al. (1998). In vitro techniques for the assessment of neurotoxicity. *Environmental health perspectives*, 106 Suppl 1:131–158.
- Hill, Jeremy D.; Zuluaga-Ramirez, Viviana; Gajghate, Sachin; Winfield, Malika; Persidsky, Yuri (2018). Activation of GPR55 increases neural stem cell proliferation and promotes early adult hippocampal neurogenesis. *British journal of pharmacology*, 175 (16):3407–3421.
- Howlett, A. C.; Barth, F.; Bonner, T. I.; Cabral, G.; Casellas, P.; Devane, W. A. et al. (2002). International Union of Pharmacology. XXVII. Classification of cannabinoid receptors. *Pharmacological reviews*, 54 (2):161–202.
- Iannotti, Fabio Arturo; Hill, Charlotte L.; Leo, Antonio; Alhusaini, Ahlam; Soubrane, Camille; Mazzearella, Enrico et al. (2014). Nonpsychotropic plant cannabinoids, cannabidivarin (CBDV) and cannabidiol (CBD), activate and desensitize transient receptor potential vanilloid 1 (TRPV1) channels in vitro: potential for the treatment of neuronal hyperexcitability. *ACS chemical neuroscience*, 5 (11):1131–1141.
- Jha, Mithilesh Kumar; Morrison, Brett M. (2018). Glia-neuron energy metabolism in health and diseases: New insights into the role of nervous system metabolic transporters. *Experimental neurology*, 309:23–31.
- Kalani, Komal; Yan, Shi Fang; Yan, Shirley ShiDu (2018). Mitochondrial permeability transition pore: a potential drug target for neurodegeneration. *Drug discovery today*, 23 (12):1983–1989.
- Kauer, Julie A.; Malenka, Robert C. (2007). Synaptic plasticity and addiction. *Nature reviews. Neuroscience*, 8 (11):844–858.

- Kaur, Gurvinder; Dufour, Jannette M. (2012). Cell lines: Valuable tools or useless artifacts. *Spermatogenesis*, 2 (1):1–5.
- Korga, Agnieszka; Ostrowska, Marta; Iwan, Magdalena; Herbet, Mariola; Dudka, Jaroslaw (2019). Inhibition of glycolysis disrupts cellular antioxidant defense and sensitizes HepG2 cells to doxorubicin treatment. *FEBS open bio*, 9 (5):959–972.
- Lambert, Didier M. (2009). *Cannabinoids in Nature and Medicine*. Weinheim, Cambridge: Wiley-VCH.
- Le, Anne; Cooper, Charles R.; Gouw, Arvin M.; Dinavahi, Ramani; Maitra, Anirban; Deck, Lorraine M. et al. (2010). Inhibition of lactate dehydrogenase A induces oxidative stress and inhibits tumor progression. *Proceedings of the National Academy of Sciences of the United States of America*, 107 (5):2037–2042.
- Leibniz Institute DSMZ. German Collection of Microorganisms and Cell Cultures GmbH. N18TG2 cell line, <https://www.dsmz.de/collection/catalogue/details/culture/ACC-103>, accessed on 30/04/2020.
- Liberti, Maria V.; Locasale, Jason W. (2016). The Warburg Effect: How Does it Benefit Cancer Cells? *Trends in biochemical sciences*, 41 (3):211–218.
- Ligresti, Alessia; Moriello, Aniello Schiano; Starowicz, Katarzyna; Matias, Isabel; Pisanti, Simona; Petrocellis, Luciano de et al. (2006). Antitumor activity of plant cannabinoids with emphasis on the effect of cannabidiol on human breast carcinoma. *The Journal of pharmacology and experimental therapeutics*, 318 (3):1375–1387.
- Liu, Q-R; Pan, C-H; Hishimoto, A.; Li, C-Y; Xi, Z-X; Llorente-Berzal, A. et al. (2009). Species differences in cannabinoid receptor 2 (CNR2 gene): identification of novel human and rodent CB2 isoforms, differential tissue expression and regulation by cannabinoid receptor ligands. *Genes, brain, and behavior*, 8 (5):519–530.
- Maccarrone, Mauro; Guzmán, Manuel; Mackie, Ken; Doherty, Patrick; Harkany, Tibor (2014). Programming of neural cells by (endo)cannabinoids: from physiological rules to emerging therapies. *Nature reviews. Neuroscience*, 15 (12):786–801.
- Magistretti, Pierre J.; Allaman, Igor (2015). A cellular perspective on brain energy metabolism and functional imaging. *Neuron*, 86 (4):883–901.

- Massi, P.; Vaccani, A.; Bianchessi, S.; Costa, B.; Macchi, P.; Parolaro, D. (2006). The non-psychoactive cannabidiol triggers caspase activation and oxidative stress in human glioma cells. *Cellular and molecular life sciences : CMLS*, 63 (17):2057–2066.
- Massi, P.; Valenti, M.; Vaccani, A.; Gasperi, V.; Perletti, G.; Marras, E. et al. (2008). 5-Lipoxygenase and anandamide hydrolase (FAAH) mediate the antitumor activity of cannabidiol, a non-psychoactive cannabinoid. *Journal of neurochemistry*, 104 (4):1091–1100.
- Massi, Paola; Solinas, Marta; Cinquina, Valentina; Parolaro, Daniela (2013). Cannabidiol as potential anticancer drug. *British journal of clinical pharmacology*, 75 (2):303–312.
- Massi, Paola; Vaccani, Angelo; Ceruti, Stefania; Colombo, Arianna; Abbracchio, Maria P.; Parolaro, Daniela (2004). Antitumor effects of cannabidiol, a nonpsychoactive cannabinoid, on human glioma cell lines. *The Journal of pharmacology and experimental therapeutics*, 308 (3):838–845.
- McAllister, Sean D.; Christian, Rigel T.; Horowitz, Maxx P.; Garcia, Amaia; Desprez, Pierre-Yves (2007). Cannabidiol as a novel inhibitor of Id-1 gene expression in aggressive breast cancer cells. *Molecular cancer therapeutics*, 6 (11):2921–2927.
- McAllister, Sean D.; Murase, Ryuichi; Christian, Rigel T.; Lau, Darryl; Zielinski, Anne J.; Allison, Juanita et al. (2011). Pathways mediating the effects of cannabidiol on the reduction of breast cancer cell proliferation, invasion, and metastasis. *Breast cancer research and treatment*, 129 (1):37–47.
- McKallip, Robert J.; Jia, Wentao; Schlomer, Jerome; Warren, James W.; Nagarkatti, Prakash S.; Nagarkatti, Mitzi (2006). Cannabidiol-induced apoptosis in human leukemia cells: A novel role of cannabidiol in the regulation of p22phox and Nox4 expression. *Molecular pharmacology*, 70 (3):897–908.
- Mergenthaler, Philipp; Lindauer, Ute; Dienel, Gerald A.; Meisel, Andreas (2013). Sugar for the brain: the role of glucose in physiological and pathological brain function. *Trends in neurosciences*, 36 (10):587–597.
- Murillo-Rodríguez, Eric; Palomero-Rivero, Marcela; Millán-Aldaco, Diana; Mechoulam, Raphael; Drucker-Colín, René (2011). Effects on sleep and dopamine levels of microdialysis perfusion of cannabidiol into the lateral hypothalamus of rats. *Life sciences*, 88 (11-12):504–511.

National Center for Biotechnology Information. PubChem Database. Arachidonic acid: CID=444899, <https://pubchem.ncbi.nlm.nih.gov/compound/444899>, accessed on 19/03/2020.

National Center for Biotechnology Information. ID1 inhibitor of DNA binding 1, HLH protein [Homo sapiens (human)] - Gene - NCBI, <https://www.ncbi.nlm.nih.gov/gene/3397>, accessed on 02/04/2020.

Norris, Christopher; Loureiro, Michael; Kramar, Cecilia; Zunder, Jordan; Renard, Justine; Rushlow, Walter; Laviolette, Steven R. (2016). Cannabidiol Modulates Fear Memory Formation Through Interactions with Serotonergic Transmission in the Mesolimbic System. *Neuropsychopharmacology : official publication of the American College of Neuropsychopharmacology*, 41 (12):2839–2850.

Olivas-Aguirre, Miguel; Torres-López, Liliana; Valle-Reyes, Juan Salvador; Hernández-Cruz, Arturo; Pottosin, Igor; Dobrovinskaya, Oxana (2019). Cannabidiol directly targets mitochondria and disturbs calcium homeostasis in acute lymphoblastic leukemia. *Cell death & disease*, 10 (10):779.

Pertwee, R. G. (2008). The diverse CB1 and CB2 receptor pharmacology of three plant cannabinoids: delta9-tetrahydrocannabinol, cannabidiol and delta9-tetrahydrocannabivarin. *British journal of pharmacology*, 153 (2):199–215.

Pertwee, R. G. (2014). Handbook of cannabis. First edition. Oxford: Oxford University Press.

Phong, Wai Yee; Lin, Wenwei; Rao, Srinivasa P. S.; Dick, Thomas; Alonso, Sylvie; Pethe, Kevin (2013). Characterization of phosphofructokinase activity in Mycobacterium tuberculosis reveals that a functional glycolytic carbon flow is necessary to limit the accumulation of toxic metabolic intermediates under hypoxia. *PloS one*, 8 (2):e56037.

Pretzsch, Charlotte Marie; Freyberg, Jan; Voinescu, Bogdan; Lythgoe, David; Horder, Jamie; Mendez, Maria Andreina et al. (2019). Effects of cannabidiol on brain excitation and inhibition systems; a randomised placebo-controlled single dose trial during magnetic resonance spectroscopy in adults with and without autism spectrum disorder. *Neuropsychopharmacology : official publication of the American College of Neuropsychopharmacology*, 44 (8):1398–1405.

PubChem. Thioguanine, <https://pubchem.ncbi.nlm.nih.gov/compound/Thioguanine>, accessed on 30/04/2020.

- Ramer, Robert; Merkord, Jutta; Rohde, Helga; Hinz, Burkhard (2010a). Cannabidiol inhibits cancer cell invasion via upregulation of tissue inhibitor of matrix metalloproteinases-1. *Biochemical pharmacology*, 79 (7):955–966.
- Ramer, Robert; Rohde, Anja; Merkord, Jutta; Rohde, Helga; Hinz, Burkhard (2010b). Decrease of plasminogen activator inhibitor-1 may contribute to the anti-invasive action of cannabidiol on human lung cancer cells. *Pharmaceutical research*, 27 (10):2162–2174.
- Ratano, Patrizia; Petrella, Carla; Forti, Fabrizio; Passeri, Pamela Petrocchi; Morena, Maria; Palmery, Maura et al. (2018). Pharmacological inhibition of 2-arachidonoylglycerol hydrolysis enhances memory consolidation in rats through CB2 receptor activation and mTOR signaling modulation. *Neuropharmacology*, 138:210–218.
- Resstel, Leonardo B. M.; Tavares, Rodrigo F.; Lisboa, Sabrina F. S.; Joca, Sâmia R. L.; Corrêa, Fernando M. A.; Guimarães, Francisco S. (2009). 5-HT<sub>1A</sub> receptors are involved in the cannabidiol-induced attenuation of behavioural and cardiovascular responses to acute restraint stress in rats. *British journal of pharmacology*, 156 (1):181–188.
- Rimmerman, N.; Ben-Hail, D.; Porat, Z.; Juknat, A.; Kozela, E.; Daniels, M. P. et al. (2013). Direct modulation of the outer mitochondrial membrane channel, voltage-dependent anion channel 1 (VDAC1) by cannabidiol: a novel mechanism for cannabinoid-induced cell death. *Cell death & disease*, 4:e949.
- Ryberg, E.; Larsson, N.; Sjögren, S.; Hjorth, S.; Hermansson, N-O; Leonova, J. et al. (2007). The orphan receptor GPR55 is a novel cannabinoid receptor. *British journal of pharmacology*, 152 (7):1092–1101.
- Salah Mohamed El Sayed; Hussam H. Baghdadi; Nassar Ayoub Abdellatif Omar; Amal Nor Edeen Ahmad Allithy; Nahed Mohammed Hablas; Ahmed Ragab Fakhreldin et al. (2018). The Antioxidant Glycolysis Inhibitor (Citric Acid) Induces a Dose-dependent Caspase-mediated Apoptosis and Necrosis in Glioma Cells. *Journal of Cancer Research and Treatment*, 6 (1):18–24.
- Shibasaki, Koji (2016). Physiological significance of TRPV2 as a mechanosensor, thermosensor and lipid sensor. *The journal of physiological sciences : JPS*, 66 (5):359–365.

- Shoshan-Barmatz, Varda; Ben-Hail, Danya (2012). VDAC, a multi-functional mitochondrial protein as a pharmacological target. *Mitochondrion*, 12 (1):24–34.
- Shoshan-Barmatz, Varda; Maldonado, Eduardo N.; Krelin, Yakov (2017). VDAC1 at the crossroads of cell metabolism, apoptosis and cell stress. *Cell stress*, 1 (1):11–36.
- Shrivastava, Ashutosh; Kuzontkoski, Paula M.; Groopman, Jerome E.; Prasad, Anil (2011). Cannabidiol induces programmed cell death in breast cancer cells by coordinating the cross-talk between apoptosis and autophagy. *Molecular cancer therapeutics*, 10 (7):1161–1172.
- Singh, Namrata; Hroudová, Jana; Fišar, Zdeněk (2015). Cannabinoid-Induced Changes in the Activity of Electron Transport Chain Complexes of Brain Mitochondria. *Journal of molecular neuroscience : MN*, 56 (4):926–931.
- Solinas, Marta; Massi, Paola; Cinquina, Valentina; Valenti, Marta; Bolognini, Daniele; Gariboldi, Marzia et al. (2013). Cannabidiol, a non-psychoactive cannabinoid compound, inhibits proliferation and invasion in U87-MG and T98G glioma cells through a multitarget effect. *PloS one*, 8 (10):e76918.
- Sugiura, Takayuki; Kishimoto, Seishi; Oka, Saori; Gokoh, Maiko (2006). Biochemistry, pharmacology and physiology of 2-arachidonoylglycerol, an endogenous cannabinoid receptor ligand. *Progress in lipid research*, 45 (5):405–446.
- Tomolonis, Julie A.; Agarwal, Saurabh; Shohet, Jason M. (2018). Neuroblastoma pathogenesis: deregulation of embryonic neural crest development. *Cell and tissue research*, 372 (2):245–262.
- UniProt. GPR55 - G-protein coupled receptor 55 - Homo sapiens (Human) - GPR55 gene & protein, <https://www.uniprot.org/uniprot/Q9Y2T6>, accessed on 22/03/2020.
- UniProt. PPARA - Peroxisome proliferator-activated receptor alpha - Homo sapiens (Human) - PPARA gene & protein, <https://www.uniprot.org/uniprot/Q07869>, accessed on 22/03/2020.
- UniProt. PPARG - Peroxisome proliferator-activated receptor gamma - Homo sapiens (Human) - PPARG gene & protein, <https://www.uniprot.org/uniprot/P37231>, accessed on 22/03/2020.

- UniProt. TRPA1 - Transient receptor potential cation channel subfamily A member 1 - Homo sapiens (Human) - TRPA1 gene & protein, <https://www.uniprot.org/uniprot/O75762>, accessed on 13/04/2020.
- UniProt. TRPV1 - Transient receptor potential cation channel subfamily V member 1 - Homo sapiens (Human) - TRPV1 gene & protein, <https://www.uniprot.org/uniprot/Q8NER1>, accessed on 22/03/2020.
- Unterberger, Alexander (2016). Neuroprotective effects of phytocannabinoids: effects of THC against radical induced oxidative stress and influences of CBD and THC on mitochondrial function. Master thesis. Vienna: University of Veterinary Medicine.
- Vaccani, Angelo; Massi, Paola; Colombo, Arianna; Rubino, Tiziana; Parolaro, Daniela (2005). Cannabidiol inhibits human glioma cell migration through a cannabinoid receptor-independent mechanism. *British journal of pharmacology*, 144 (8):1032–1036.
- Voet, Donald; Voet, Judith G.; Maelicke, Alfred; Börsch-Supan, Martina (1992). *Biochemie*. Weinheim, New York: VCH.
- Vogel, Timothy W.; Zhuang, Zhengping; Li, Jie; Okamoto, Hiroaki; Furuta, Makoto; Lee, Youn-Soo et al. (2005). Proteins and protein pattern differences between glioma cell lines and glioblastoma multiforme. *Clinical cancer research : an official journal of the American Association for Cancer Research*, 11 (10):3624–3632.
- Williams, C. M.; Kirkham, T. C. (1999). Anandamide induces overeating: mediation by central cannabinoid (CB1) receptors. *Psychopharmacology*, 143 (3):315–317.
- Wu, Hsin-Ying; Huang, Chung-Hsiung; Lin, Yi-Hsuan; Wang, Chia-Chi; Jan, Tong-Rong (2018). Cannabidiol induced apoptosis in human monocytes through mitochondrial permeability transition pore-mediated ROS production. *Free radical biology & medicine*, 124:311–318.
- Zhang, Dongsheng; Li, Juan; Wang, Fengzhen; Hu, Jun; Wang, Shuwei; Sun, Yueming (2014). 2-Deoxy-D-glucose targeting of glucose metabolism in cancer cells as a potential therapy. *Cancer letters*, 355 (2):176–183.
- Zhornitsky, Simon; Potvin, Stéphane (2012). Cannabidiol in humans-the quest for therapeutic targets. *Pharmaceuticals (Basel, Switzerland)*, 5 (5):529–552.

## 8. Appendix

### 8.1. Figure Index

Figure 1. Activation of presynaptic CB <sub>1</sub> receptors leads to weakening of synaptic transmission (Kauer and Malenka 2007)	6
Figure 2. All 5 known endocannabinoids (Bisogno 2008)	7
Figure 3. Structure of CBD (Massi et al. 2013)	9
Figure 4. Western Blot Analysis of the expression of Id-1 with CBD at concentrations of 0.1, 1.0 & 1.5 µmol/l (McAllister et al. 2007)	11
Figure 5. Tumour size of inoculated A549 lung cancer cells after treatment with CBD or a vehicle for up to 42 days (Ramer et al. 2010b)	12
Figure 6. Effects of CBD on glioma cells (Massi et al. 2013)	13
Figure 7. Anatomical structures of the mesolimbic system (Arias-Carrión et al. 2010)	14
Figure 8. Western Blot Analysis of the amount of cytochrome c released into the cytosol of monocytes (Wu et al. 2018)	15
Figure 9. Overview of glycolysis (adapted from Phong et al. 2013)	17
Figure 10. Overview of CAC (adapted from Salah Mohamed El Sayed et al. 2018)	17
Figure 11. Overview of oxidative phosphorylation (adapted from Benard et al. 2011)	18
Figure 12. Comparison between glucose and 2-DG (adapted from Aghaee et al. 2012)	19
Figure 13. Reduction of resazurin into resorufin by viable cells (Creative Bioarray 22/04/2020)	33
Figure 14. LDH activity in U-87 MG glioma after exposure to 2-DG for (a) 24 hours and (b) 48 hours. Data are expressed as means ± SD of 4 independent experiments. Statistical evaluation does not reveal any significant changes.	35

Figure 15. Resazurin reduction in U-87 MG glioma after exposure to 2-DG for (a) 24 hours and (b) 48 hours. Data are expressed as means  $\pm$  SD of 4 independent experiments.  $P < 0.05$  (\*) determined with Kruskal-Wallis (H)-test followed by Chi<sup>2</sup>-test. 36

Figure 16. Protein content in U-87 MG glioma after exposure to 2-DG for (a) 24 hours and (b) 48 hours. Data are expressed as means  $\pm$  SD of 4 independent experiments.  $P < 0.05$  (\*) determined with Kruskal-Wallis (H)-test followed by Chi<sup>2</sup>-test. 37

Figure 17. LDH activity in N18TG2 neuroblastoma after exposure to 2-DG for (a) 24 hours and (b) 48 hours. Data are expressed as means  $\pm$  SD of 4 independent experiments. Statistical evaluation does not reveal any significant changes. 38

Figure 18. Resazurin reduction in N18TG2 neuroblastoma after exposure to 2-DG for (a) 24 hours and (b) 48 hours. Data are expressed as means  $\pm$  SD of 4 independent experiments.  $P < 0.05$  (\*) determined with Kruskal-Wallis (H)-test followed by Chi<sup>2</sup>-test. 39

Figure 19. Protein content in N18TG2 neuroblastoma after exposure to 2-DG for (a) 24 hours and (b) 48 hours. Data are expressed as means  $\pm$  SD of 4 independent experiments.  $P < 0.05$  (\*) determined with Kruskal-Wallis (H)-test followed by Chi<sup>2</sup>-test. 40

Figure 20. Comparison between N18TG2 neuroblastoma and U-87 MG glioma regarding resazurin reduction normalized to protein content after exposure to 2-DG for (a) 24 hours and (b) 48 hours. Data are expressed as means  $\pm$  SD of 4 independent experiments.  $P < 0.05$  (\*) determined with Kruskal-Wallis (H)-test followed by Chi<sup>2</sup>-test. 41

Figure 21. LDH activity in U-87 MG glioma after exposure to CBD for (a) 24 hours and (b) 48 hours. Data are expressed as means  $\pm$  SD of 4 independent experiments. Statistical evaluation does not reveal any significant changes. 42

Figure 22. Resazurin reduction in U-87 MG glioma after exposure to CBD for (a) 24 hours and (b) 48 hours. Data are expressed as means  $\pm$  SD of 4 independent experiments. Statistical evaluation does not reveal any significant changes. 43

Figure 23. Protein content in U-87 MG glioma after exposure to CBD for (a) 24 hours and (b) 48 hours. Data are expressed as means  $\pm$  SD of 4 independent experiments. Statistical evaluation does not reveal any significant changes. 44

Figure 24. LDH activity in N18TG2 neuroblastoma after exposure to CBD for (a) 24 hours and (b) 48 hours. Data are expressed as means  $\pm$  SD of 4 independent experiments. Statistical evaluation does not reveal any significant changes. 45

Figure 25. Resazurin reduction in N18TG2 neuroblastoma after exposure to CBD for (a) 24 hours and (b) 48 hours. Data are expressed as means  $\pm$  SD of 4 independent experiments.  $P < 0.05$  (\*) determined with Kruskal-Wallis (H)-test followed by Chi<sup>2</sup>-test. 46

Figure 26. Protein content in N18TG2 neuroblastoma after exposure to CBD for (a) 24 hours and (b) 48 hours. Data are expressed as means  $\pm$  SD of 4 independent experiments.  $P < 0.05$  (\*) determined with Kruskal-Wallis (H)-test followed by Chi<sup>2</sup>-test. 47

Figure 27. Comparison between N18TG2 neuroblastoma and U-87 MG glioma regarding resazurin reduction normalized to protein content after exposure to CBD for (a) 24 hours and (b) 48 hours. Data are expressed as means  $\pm$  SD of 4 independent experiments. Statistical evaluation does not reveal any significant changes. 48

Figure 28. LDH activity in U-87 MG glioma after exposure to CBD and 10 mM 2-DG for (a) 24 hours and (b) 48 hours. Data are expressed as means  $\pm$  SD of 4 independent experiments. Statistical evaluation does not reveal any significant changes. 49

Figure 29. Resazurin reduction in U-87 MG glioma after exposure to CBD and 10 mM 2-DG for (a) 24 hours and (b) 48 hours. Data are expressed as means  $\pm$  SD of 4 independent experiments.  $P < 0.05$  (#) determined with Mann-Whitney-U-test for comparison between the control group and the group that was treated with 2-DG. 50

Figure 30. Protein content in U-87 MG glioma after exposure to CBD and 10 mM 2-DG for (a) 24 hours and (b) 48 hours. Data are expressed as means  $\pm$  SD of 4 independent experiments.  $P < 0.05$  (#) determined with Mann-Whitney-U-test for comparison between the control group and the group that was treated with 2-DG. 51

Figure 31. LDH activity in N18TG2 neuroblastoma after exposure to CBD and 10 mM 2-DG for (a) 24 hours and (b) 48 hours. Data are expressed as means  $\pm$  SD of 6 independent experiments. Statistical evaluation does not reveal any significant changes. 52

Figure 32. Resazurin reduction in N18TG2 neuroblastoma after exposure to CBD and 10 mM 2-DG for (a) 24 hours and (b) 48 hours. Data are expressed as means  $\pm$  SD of 6 independent experiments.  $P < 0.05$  (#) determined with Kruskal Mann-Whitney-U-test for comparison between the control group and the group that was treated with 2-DG. 53

Figure 33. Protein content in N18TG2 neuroblastoma after exposure to CBD and 10 mM 2-DG for (a) 24 hours and (b) 48 hours. Data are expressed as means  $\pm$  SD of 6 independent experiments.  $P < 0.05$  (#) determined with Mann-Whitney-U-test for comparison between the control group and the group that was treated with 2-DG. 54

Figure 34. Comparison between N18TG2 neuroblastoma and U-87 MG glioma regarding resazurin reduction normalized to protein content after exposure to CBD and 10 mM 2-DG for (a) 24 hours and (b) 48 hours. Data are expressed as means  $\pm$  SD of 6 independent experiments with N18TG2 neuroblastoma cells and 4 independent experiments with U-87 MG glioma cells.  $P < 0.05$  (#) determined with Mann-Whitney-U-test for comparison between the control group and the group that was treated with 2-DG. 55

Figure 35. Number of TH-positive murine primary cells after exposure to 2-DG. Data are expressed as means  $\pm$  SD of 1 experiment. Statistical evaluation cannot be compiled. 56

## 8.2. Table Index

Table 1. Constituents of <i>Cannabis sativa</i> by chemical class (adapted from Pertwee 2014)	8
Table 2. Overview of how the required equipment and solutions were prepared for the preparation of the pregnant mouse	25
Table 3. Composition of BM and N4	27
Table 4. Overview of how mesencephalic primary cells were cultivated for 15 days	27
Table 5. Composition of MM and TM	29
Table 6. Overview of how cells were seeded for the determination of the toxicity of 2-DG	30
Table 7. The tested dilutions of 2-DG	30
Table 8. Overview of how cells were seeded for the CBD-experiment	31
Table 9. The tested dilutions of CBD	31
Table 10. The appropriate 2-DG dilution for the CBD-experiment	32
Table 11. Overview of how chemicals were prepared for the determination of LDH activity	32

Table 12. Composition of WR for BCA-Protein Assay	34
Table 13. Composition of standard probes for BCA-Protein Assay	34

### 8.3. Abbreviations

2-AG.....	2-arachidonoylglycerol
2-DG .....	2-deoxy-D-glucose
5-HT1a .....	5-hydroxytryptamine receptor 1A
5-LO .....	5-lipoxygenase
6-HD.....	6-hydroxydopamine
acetyl-CoA.....	acetyl coenzyme A
AD .....	Alzheimer's Disease
ADCY .....	adenylyl cyclase
anandamide .....	N-arachidonylethanolamine
ANLS.....	astrocyte-to-neuron lactate shuttle
ATP .....	adenosine triphosphate
BCA.....	bicinchoninic acid
BM.....	basic medium
BSA.....	bovine serum albumin
CAC .....	citric acid cycle
cAMP .....	cyclic adenosine monophosphate
CB <sub>1</sub> .....	cannabinoid receptor type-1
CB <sub>2</sub> .....	cannabinoid receptor type-2
CBD .....	cannabidiol
cDMEM .....	colourless Dulbecco's modified eagle's medium
CM .....	control medium
CNS .....	central nervous system
CYP.....	cytochrome P450 enzyme

DAB.....	3,3'-diaminobenzidinetetrahydrochloride-hydrate
DMEM .....	Dulbecco's modified eagle's medium
DMSO .....	dimethyl sulfoxide
DPBS .....	Dulbecco's modified phosphate buffered saline
ERK.....	extracellular signal-regulated kinase
FAAH .....	fatty acid amide hydrolase
FADH <sub>2</sub> .....	flavin adenine dinucleotide
GABA .....	γ-aminobutyric acid
GPR55 .....	G-protein coupled receptor 55
GTP.....	guanosine triphosphate
H <sub>2</sub> O <sub>2</sub> .....	hydrogen peroxide
HBSS .....	Hank's balanced salt solution
HLH.....	helix-loop-helix
i.p. ....	intraperitoneal
LDH.....	lactate dehydrogenase
MAPK.....	mitogen-activated protein kinase
MM.....	maintaining-medium
MPTP .....	mitochondrial permeability transition pore
NADH.....	nicotinamide adenine dinucleotide
Na-pyruvate.....	sodium-pyruvate
PD .....	Parkinson's Disease
PDH .....	pyruvate dehydrogenase
PDL .....	poly-D-lysine hydrobromide
PNS.....	peripheral nervous system
PPARα .....	peroxisome proliferator-activated receptor α
PPARγ .....	peroxisome proliferator-activated receptor γ
ROS .....	reactive oxygen species

s.c.	subcutaneous
SD	standard deviation
TH	tyrosine-hydroxylase
TIMP1	tissue inhibitor of matrix metalloproteinases-1
TM	treatment-medium
TNF $\alpha$	tumor necrosis factor $\alpha$
TRPA1	transient receptor potential cation channel subfamily A member 1
TRPV1	transient receptor potential cation channel subfamily 5 member 1
TRPV2	transient receptor potential cation channel subfamily 5 member 2
VDAC	voltage-dependent anion channel
WR	working reagent
$\Delta^9$ -THC	(-)-delta-9-trans-tetrahydrocannabinol